Effects of periodic bottlenecks on the dynamics of adaptive evolution in microbial populations

Minako Izutsu[a,b,c, *,1], Devin M. Lake[b,c,d,1], Zachary W. D. Matson[e], Jack P. Dodson[a], and Richard E. Lenski[a,b,c,d,*]

[a]Department of Microbiology and Molecular Genetics, Michigan State University, East Lansing, MI 48824; [b]BEACON Center for the Study of Evolution in Action, Michigan State University, East Lansing, MI 48824; [c]Ecology, Evolutionary Biology and Behavior Program, Michigan State University, East Lansing, MI 48824; [d]Department of Integrative Biology; and [e]Department of Computer Science and Engineering, Michigan State University, East Lansing, MI 48824

Abstract

Population bottlenecks are common in nature, and they can impact the rate of adaptation in evolving populations. On the one hand, each bottleneck reduces the genetic variation that fuels adaptation. On the other hand, fewer founders can undergo more generations and leave more descendants in a resource-limited environment, which allows surviving beneficial mutations to spread more quickly. Here we investigate the impact of repeated bottlenecks on the dynamics of adaptation in experimental populations of *Escherichia coli*. We propagated 48 populations under four dilution regimes (2-, 8-, 100-, and 1000-fold), all reaching the same final size each day, for 150 days. A simple model in which adaptation is limited by the supply rate of beneficial mutations predicts that fitness gains should be maximized with ~8-fold dilutions. The model also assumes that selection acts only on the overall growth rate and is otherwise identical across dilution regimes. However, we found that selection in the 2-fold regime was qualitatively different from the other treatments. Moreover, we observed earlier and greater fitness gains in the populations subjected to 100- and 1000-fold dilutions than in those that evolved in the 8-fold regime. We also ran

simulations using parameters estimated independently from a long-term experiment using the same ancestral strain and environment. The simulations produced dynamics similar to our empirical results under these regimes, and they indicate that the simple model fails owing to the assumption that the supply of beneficial mutations limits adaptation.

adaptation | clonal interference | experimental evolution | mutation supply | population bottleneck

Significance

Many microorganisms experience population "bottlenecks" during transmission between hosts or when propagated in the laboratory. These bottlenecks reduce genetic variation, potentially impeding natural selection. However, bottlenecks can also increase the number of generations over which selection acts, potentially accelerating adaptation. We explored this tension by propagating 48 bacterial populations for 150 days under regimes in which they were diluted 2-, 8-, 100-, or 1000-fold each day. On balance, the bacteria evolved earlier and adapted faster at the higher dilutions. These results contradict theory that accounts for the loss of genetic variation at higher dilutions, but not for the increased number of generations. We also performed simulations that reflect these opposing factors, and the simulations agree well with our experimental results.

Data deposition: All of the data and analysis scripts used in this study will be deposited in the Dryad Digital Repository upon acceptance (doi: TO BE ADDED).

Author contributions: M.I., D.M.L., and R.E.L. designed research; M.I. and J.P.D. performed experiments; D.M.L., Z.W.D.M., and R.E.L. performed simulations; M.I., D.M.L., and R.E.L. analyzed data; and M.I., D.M.L., and R.E.L. wrote the paper.

This article contains supporting information online at TO BE ADDED.

[*] To whom correspondence may be addressed. Email: izutsumi@msu.edu or lenski@msu.edu.

[1] These authors contributed equally to the work.

Introduction

Population sizes often fluctuate in time, sometimes greatly, with important effects on evolution (1, 2). A bottleneck occurs when a population's size drops suddenly, often leading to the loss of some genetic variants and a concomitant increase in frequency or even fixation of other variants. Bottlenecks occur in a variety of contexts, with some important distinctions including (i) whether the survivors of a bottleneck are a random subset of the previous population or possess some particular trait (e.g., resistance to a selective agent); and (ii) whether a bottleneck and subsequent recovery are singular events or occur periodically (e.g., seasonally). Our focus here is on periodic bottlenecks in which the survivors are a random subset of the previous population. This situation arises with the serial transfer protocols used in many evolution experiments (3–5), and it is similar to the transmission of microbial pathogens and commensals between hosts (6–9). Therefore, understanding the effects of periodic population bottlenecks is not only of interest in evolutionary theory, but also for understanding the adaptation of microbes to their hosts.

In the case of extreme bottlenecks, a population's mean fitness can decline over time, even in a constant environment. For example, in mutation-accumulation experiments, lineages are repeatedly propagated via single-cell bottlenecks, in the case of microbes, or full-sibling crosses, in the case of sexual organisms, thereby purging all or most genetic variation and preventing natural selection from acting (except against lethal or nearly lethal variants, which are not detected and so cannot be propagated). New mutations still arise in these experiments, but in the absence of selection populations accumulate mutations without regard to their fitness effects; and because more mutations are deleterious than beneficial, the accumulation of these random mutations causes fitness to decline over time (10–12).

In this study, we are concerned with less severe bottlenecks, which nonetheless can have

important consequences for the dynamics of adaptation. In particular, we consider populations of asexual organisms that are propagated via periodic (e.g., daily) serial transfers into fresh medium. We consider cases in which the organisms can grow fast enough that, regardless of the dilution imposed, the population depletes the limiting resource before the next dilution takes place. The population thus reaches a final stationary-phase density, and we assume for simplicity that no death or other changes in growth potential occur prior to the next transfer. The situation described above closely matches the long-term evolution experiment (LTEE) with *Escherichia coli* that has been running for over 30 years and 70,000 generations (3, 12–14). Each day in the LTEE, the bacteria are diluted 100-fold into 10 mL of fresh medium, with glucose as the limiting resource. The glucose concentration allows the bacteria to reach a final density of ~5 x 10^7 cells per mL, or ~5 x 10^8 cells in total. After each dilution, the population then grows 100-fold to reach stationary phase. That regrowth corresponds to $\log_2 100 \approx 6.6$ doublings per day. In this medium, the ancestral bacteria grow with a doubling time of ~1 h, and so they readily reach the final density well before the next dilution and transfer. Indeed, they could be diluted a million-fold and still achieve the 20 doublings required to reach stationary phase. Depending on the particular strain and culture medium, some bacteria might experience death after they exhaust their resources. However, in the case of the ancestral strain and culture conditions used in the LTEE, there is little or no cell death between transfers (15).

We ask the following question: What daily dilution factor, D, maximizes the rate of fitness gain? To address this question, we performed experiments and numerical simulations, which take advantage of the knowledge gained from the LTEE, including previous estimates of the beneficial mutation rate, distribution of fitness effects associated with beneficial mutations, and so on (13). The ancestral strain used in the LTEE has a low point-mutation rate, on the order of 10^{-10} per base

pair and ~10^{-3} across the entire genome (12, 16). Also, the dilution regimes in our experiments are such that the minimum population size is >10^5 cells even in the most severe bottleneck treatment. Given the low mutation rate and large minimum size, our simulations ignore the fixation of deleterious mutations and instead focus on the effects of varying D on the survival and spread of beneficial mutations. For the purpose of theoretical predictions and numerical simulations, we assume that nothing else changes about the environment and the parameters governing selection when we vary D. In our experiments, however, we examine whether this assumption might be violated.

Given the simplifying assumptions outlined above, changing the dilution factor has two opposing effects. On the one hand, a more severe bottleneck will cause the loss by drift of a higher proportion of beneficial mutations soon after they arise and while they are still at low frequencies, resulting in fewer surviving beneficial mutations (Fig. 1, solid curve). On the other hand, a more severe bottleneck also means that more generations occur each day prior to dilution and transfer, thereby amplifying the growth advantage of those beneficial mutations that survive the bottlenecks (Fig. 1, dashed line). Wahl et al. (4) presented a model corresponding to this scenario in order to derive the dilution factor that maximizes the supply of beneficial mutations that survive periodic bottlenecks. According to their analysis, the supply of surviving beneficial mutations is maximized when $D = e^2 \approx 7.4$. We confirmed their result using a different derivation (Supplemental Text). If the supply of surviving beneficial mutations limits the speed of adaptive evolution—in essence, a strong-selection, weak-mutation regime (17, 18)—then that same dilution factor should also maximize the rate of fitness increase. However, as will show, this analysis does not account for the number of generations between transfers, which determines the speed at which the surviving beneficial mutations can spread through an evolving population. Thus, the dilution factor that

maximizes the rate of fitness increase when beneficial mutations are common remains unclear.

Here, we report the results of experiments in which we examined the effect of different dilution regimes on the rate of adaptive evolution. To that end, we propagated 12 populations of *E. coli* under each of four daily dilution regimes (2-, 8-, 100-, and 1000-fold) for 150 days. We used the same ancestral strains and culture conditions as in the LTEE, and we performed competition assays to measure changes in the bacteria's competitive fitness. One methodological difference in our experimental setup is that each population began with an equal mixture of two ancestral strains that differ by a neutral genetic marker, whereas each LTEE population began with one or the other variant. By starting each population with a mixture of the two marked variants, and by monitoring their relative abundance over time, we could determine when a beneficial mutation began to sweep through a population, causing a shift in the ratio of the marked lineages. In addition to comparing our experimental results with the predictions of the theory of Wahl et al. (4), we performed numerical simulations across the same and other dilution regimes, using parameters estimated from the LTEE (13).

Several other recent experiments with bacteria have explored the effects of population bottlenecks on adaptive evolution (19–23). These studies employed different experimental designs from ours and addressed different questions; some imposed single rather than repeated bottlenecks, while others varied the selective environment, final population size, or both. Hence, these experiments do not answer the question that was posed by Wahl et al. (4), and which we now examine, regarding the dilution factor that maximizes the rate of fitness increase in populations experiencing periodic bottlenecks while reaching the same final population size between transfers.

Results

Marker Divergence in the Evolution Experiment. We propagated 48 populations of *E. coli* for 150 days with 2-, 8-, 100-, or 1000-fold daily dilutions of the previous day's culture into fresh medium. Each day, a population grew for $\log_2 D$ cell generations until it reached its final size, N_f, at which point the limiting glucose was exhausted. The four dilution regimes thus allowed 1, 3, ~6.6, and ~10 generations per day, respectively, over the 150-day experiment. All populations started with an equal mixture of Ara^- and Ara^+ strains that differ by a mutation that is neutral in the glucose-limited environment, but which causes the cells to form red and white colonies, respectively, when plated on tetrazolium arabinose (TA) agar (3). The ratio of the two lineages should remain constant over time, except for statistical fluctuations (primarily sampling error when only a few hundred colonies are counted), until a beneficial mutation arises and spreads through one or the other lineage. Beneficial mutations cause sustained perturbations to the ratio in a given population, but across replicate populations the direction of the perturbation should be random. Comparing the trajectories of the ratio between treatments allows us to quantify differences in the timing of the perturbations caused by beneficial mutations. Each marked lineage within a particular treatment started from an inoculum obtained by plating for single colonies (each derived from a single cell) to ensure that the replicate populations did not share any mutations that were identical by descent. However, the same two source colonies were used as founders for one population in each of the dilution treatments. We sampled each population every 3 days and spread the sample on a TA agar plate, allowing us to score cells based on whether they were descended from the Ara^- or Ara^+ founding lineage. We continued this procedure until a population appeared to have fixed one or the other marker state, after which we plated samples every 15 days.

Figure 2 shows the resulting trajectories of the $\log_2$-transformed ratio of the abundances of the marked lineages for the 12 populations under each of the dilution regimes. For 10 of the 12

replicate populations in each treatment, the ratios remained essentially constant for many days, as expected given the marker's neutrality. However, for 2 populations in each treatment, the ratio of the lineages systematically increased (grey trajectories) or decreased (mauve trajectories) from the beginning of the experiment. These deviations imply that the founding clones already harbored mutations that were not neutral. This inference is supported by the fact that the same replicates (founded from the same pair of colonies) experienced the same directional deviations in all four treatments. Having saved samples of the 24 founding colonies, we could test whether the particular clonal isolates had mutations that affected their fitness by competing them against the reciprocally marked ancestors, REL606 and REL607, in the 100-fold dilution regime. Indeed, the founding clones from the atypical populations differed significantly in their fitness (Table S1), and in the directions expected from their aberrant trajectories (Fig. 2), confirming the presence of non-neutral mutations in the founders. We therefore excluded these replicates in all four treatments from our analyses of the marker-ratio trajectories, because they violated the assumption of initial neutrality.

Time to Divergence. Inspection of the marker-ratio trajectories suggests that deviations from the initial 1:1 ratio (0 on the log-transformed scale) of the marked lineages tended to begin earlier in the populations subjected to the more severe bottlenecks (Fig. 2). To confirm that impression, we identified for each population the time to divergence, *TD*, based on when the ratio diverged from 1:1 by at least a factor of 2 (i.e., the $\log_2$ ratio deviated from 0 by 1) in either direction. One population in the 2-fold dilution treatment never deviated by as much as 2-fold from the 1:1 ratio, and we used 150 days (i.e., the duration of the experiment) as its divergence time.

Figure 3 shows that *TD* values for the 2-fold dilution regime ranged from 66 to 150 days, with a median of 78 days. For the 8-fold treatment, the values ranged from 51 to 123 days, with a median *TD* of 61.5 days. With 100-fold dilutions, *TD* values ranged from 30 to 69 days, with a

median of 39 days. In the 1000-fold regime, the median *TD* value was 33 days, with the replicate populations ranging from 24 to 33 days. All six pairwise comparisons of *TD* values between the four dilution regimes are significant (Table S2), even after a Bonferroni correction for multiple comparisons. Thus, divergence in the marker ratios occurred earlier with increasing values of the dilution factor, *D*, indicating that selective sweeps began earlier at the higher dilutions. This metric, at least, does not agree with the theoretical prediction that the intermediate 8-fold dilution regime should generate the fastest adaptive evolution (Fig. 1). Instead, the rank order of the four treatments corresponds with the cumulative number of generations over the 150-day experiment: namely, 150, 450, ~1000, and ~1500 generations for the 2-, 8-, 100-, 1000-fold dilution regimes, respectively. If we express *TD* not in days, but in generations, then the median values are 78, 185, 259, and 329 generations for the 2-, 8-, 100-, and 1000-fold dilutions, respectively. Thus, these data suggest that the more extreme dilutions promoted faster adaptation on a chronological basis, but slower on a generational basis.

Fluctuations in Marker Ratio. We also examined the magnitude of fluctuations in the marker ratio between consecutive samples through day 21 (just before the earliest 2-fold divergence in any of the 40 qualifying populations). We did so to check whether the dilution regimes produced different fluctuation patterns that might confound our use of the same criterion (i.e., a 2-fold shift in ratio of the marked lineages) to identify perturbations caused by selective sweeps of beneficial mutations. We did not expect to see different fluctuation profiles across the treatments, despite the different bottleneck sizes, because the sampling error associated with scoring a few hundred cells in a typical sample is much greater than the effect of genetic drift in populations with $>10^5$ cells even during the most severe bottleneck (i.e., $\sim 5 \times 10^7$ cells/mL × 10 mL, then diluted 1000-fold). As expected, an ANOVA shows no significant differences among the treatments (Table S3). Also,

only 3.6% (10/280) of the fluctuations were even half as large as the 2-fold change in marker ratio that we used as the cutoff to identify perturbations caused by beneficial mutations. Moreover, the initial 2-fold changes in marker ratios were generally followed by further large changes (Fig. 2), as expected for selective sweeps, but not for fluctuations caused by drift or sampling noise.

Readers who are unfamiliar with marker-divergence experiments may, on first inspection, be surprised by the reversals in the marker-ratio trajectories that occurred in some populations after the onset of a selective sweep. However, such reversals are widely observed, and indeed expected, given clonal interference between contending lineages that have independently acquired beneficial mutations (24–26). As a beneficial mutation sweeps through one marked lineage, it must compete not only against the progenitors (of both marker types) but also against any beneficial mutations that arose in the opposing lineage. If the competing mutations have similar fitness effects, then the marked lineages might appear to equilibrate at some new ratio. If the later-arising mutation is more beneficial than the one that arose first, then the marker-trajectory may reverse direction, and further reversals can occur as additional beneficial mutations arise in one or both lineages.

Fitness in Home and Away Environments. To assess the effect of bottlenecks on the extent of adaptation, we measured the fitness gains of the evolved bacteria by competing them against the ancestral strain. We could not measure the fitness of the entire evolved populations because we had to mix the evolved bacteria with the ancestral strain bearing the alternative marker to measure their relative fitness, and some populations still had descendants of both marked lineages at the end of the experiment (day 150). Instead, we isolated clones from each final population and then competed each of them against the reciprocally marked ancestor to measure their relative fitness.

We measured the fitness of each evolved clone in two conditions, which we call the “home” and “away” environments. For the former, we measured fitness using the same dilution treatment

in which the clone had evolved. For the latter, we used the 100-fold dilution regime, regardless of the treatment in which the clone had evolved. We used these environments in order to test whether any observed differences in fitness gains might reflect different selection pressures among the four dilution treatments, which would complicate interpretation of the results in relation to theoretical predictions and numerical simulations. Differences in selection might occur, for example, because the durations of the lag, growth, and stationary phases vary as a function of the dilution protocol. By contrast, the model and simulations implicitly assume that selection results from differences in growth rate only.

Figure 4 shows the relative fitness values for all of the 150-day clones, plotted as the values measured in their home environment versus in the common away environment. Most clones that evolved in the 2-fold dilution treatment were much more fit at home than away (Fig. 4A). They had an average fitness gain of ~24% with 2-fold dilutions, but only ~6% when subjected to 100-fold dilutions. These data indicate that the nature of selection differed between the 2-fold and 100-fold dilution treatments. This difference might reflect the heightened importance of shortening the lag phase relative to faster growth when there is only one doubling per day, or the fact that half of the medium contains the byproducts of metabolism and growth from the previous day at the 2-fold dilution.

The clones that evolved in the 8-fold dilution treatment also tended to be more fit in their home environment than in the common 100-fold regime, but this difference was much smaller than for the 2-fold treatment (Fig. 4B, Table S4). To see whether this difference might undermine using the common environment for comparison purposes, we measured the fitness of the evolved clones from both the 8- and 100-fold dilution treatments under the 8-fold dilution regime (Fig. S1A). The clones that evolved in the 100-fold regime had significantly higher fitness than those that evolved

in the 8-fold regime, even when the competitions were performed in the 8-fold regime ($p = 0.0342$, two-tailed Wilcoxon's signed-ranks test). Also, the fitness values measured using 8-fold and 100-fold dilutions were well correlated for the clones from both evolutionary treatments (Fig. S1B, $r = 0.7399$, $p < 0.0001$). Thus, selection in these two treatments was sufficiently similar that evolution under the 100-fold regime led to higher fitness than evolution under the 8-fold regime, regardless of the competition environment.

Therefore, the fitness gains measured in the home and away environments for the bacteria that evolved under the 8-, 100-, and 1000-fold dilution regimes are largely consistent with simple selection for faster growth. However, the bacteria that evolved in the 2-fold dilution treatment experienced substantially different selection pressures, and therefore that treatment cannot be used to test predictions based on the theoretical model and numerical simulations.

Comparison of Final Fitness Values. We ran additional competitions with 5-fold replication to obtain more accurate estimates of the final fitness levels of the populations that evolved in the 8-, 100-, and 1000-fold dilution regimes, when all were measured in the common 100-fold regime. The populations from the 100- and 1000-fold treatments were significantly more fit than those from the 8-fold treatment (Table S5), whereas there was no difference between the 100- and 1000-fold treatments. These direct measurements of fitness thus support the finding from the marker-divergence analysis that adaptation was faster under the 100- and 1000-fold dilution regimes than under the 8-fold regime, contrary to the prediction based on the supply of surviving beneficial mutations.

Rate of Fitness Improvement during Later Transfers. We now consider a possible reason for the discrepancy between the prediction that the supply of surviving beneficial mutations should be greater at $D = 8$ than at $D = 100$ or $D = 1000$, and our empirical findings that selective sweeps

started earlier (Figs. 2 and 3), and cumulative fitness gains were larger (Table S5), at the more extreme dilutions. The model predicts that more beneficial mutations will survive, and by extension that adaptation will be faster, under a quasi-steady-state scenario, whereas our experiments started without any genetic variation and hence far from a steady state. To address this issue, we measured the fitness of clones isolated after 90 transfers at the same time that we assayed the clones sampled after 150 transfers (Fig. 5). We chose 90 transfers because the ratio of the marked lineages had diverged, and thus meaningful adaptation was underway, in the three relevant treatments by that timepoint (Fig. 2). We compared the change in fitness from transfer 90 to transfer 150 among the 8-, 100-, and 1000-fold dilution treatments. We found no support for that prediction that continued adaptation would be faster at the 8-fold dilution regime. Instead, the average fitness increases were higher for both the 100- and 1000-fold treatments than for the 8-fold treatment (Fig. 5), although the differences were not statistically significant (Table S6).

Simulated Fitness Trajectories under the Four Experimental Regimes. In the sections above, we analyzed the marker-divergence trajectories and fitness assays in several ways. None of our analyses supported the prediction of faster adaptation with an intermediate dilution factor of $D = 8$ than with $D = 100$ or 1000; instead, they showed significantly earlier and greater adaptation in populations evolving at those higher dilutions. We ran simulations to gain a better understanding of this discrepancy. Our simulations tracked the abundance of every lineage with a new beneficial mutation; a lineage could go extinct either by random drift during the periodic dilutions or by being outcompeted by other lineages. Recall that the model of Wahl et al. (4) assumes a constant final population size, and that selection acts through differences in growth rate; our simulations make the same assumptions. To parameterize the simulations, we used the same final population size as in the LTEE (and our experiments) along with estimates derived from the LTEE for the rate of

beneficial mutations, the ancestral distribution of fitness effects, and the strength of diminishing-returns epistasis (13). These parameters were previously shown to describe and even predict with high accuracy the observed trajectories for fitness in the LTEE (13, 27). The simulations, like the theory of Wahl et al. (4), should account for the supply of surviving beneficial mutations. In addition, the simulations (unlike that theory) account for the subsequent rate of increase in the abundance of the surviving mutants, with higher dilution factors allowing fitness differences to compound for more generations between transfers.

We simulated the same four dilution treatments as in our experiments, and we evolved 100 replicate populations of each for 150 transfers (Fig. 6). The simulations show good agreement with the experimental results for the 8-, 100-, and 1000-fold dilution treatments. First, fitness typically started to increase slightly earlier in the simulations at $D = 1000$ than at $D = 100$, and much earlier than at $D = 8$ (Figs. 6 and S2), with the same rank order and similar times to the onset of marker divergence observed in the experimental trajectories (Figs. 2 and 3, Table S7). Second, the grand mean fitness after 150 simulated transfers was slightly higher for $D = 100$ than $D = 1000$, and both were substantially higher than $D = 8$ (Fig. 6), with the same rank order of fitness values and similar differentials as in our experiments (Fig. 5). Third, the average fitness gains between transfers 90 and 150 in the simulations were higher for $D = 100$ and $D = 1000$ than for $D = 8$ (Fig. 6, Table S8), again as seen in our experiments (Fig. 5). By contrast, the theory based on the supply of surviving beneficial mutations predicts none of these patterns; instead, it predicts a greater supply and, by extension, a faster rate of adaptive evolution at $D = 8$ than at $D = 100$, which in turn should be faster than at $D = 1000$ (Fig. 1).

The only substantive disagreement between the simulations and our experimental results involves the $D = 2$ dilution regime. The simulations predict barely perceptible fitness gains in this

regime by 150 transfers (Fig. 6), whereas we saw much larger gains by that time point, especially when fitness was measured in the home environment with the 2-fold dilution regime (Fig. 4A). The discrepancy between simulations and experiments in this case is also evident in the marker-divergence trajectories: only 2 of the 100 simulated populations had diverged by the 150th transfer (Table S7), whereas all but one of the experimental populations had diverged by then (Fig.3). However, as we showed when presenting the experimental results, the cells experienced different selection pressures in the 2-fold dilution regime than in the other treatments, and different from those assumed in the simulations. The fact that the simulated populations deviate profoundly from the experimental ones only for the 2-fold treatment therefore reinforces the non-comparability of that treatment with the others in terms of understanding the dynamical (as opposed to ecological) consequences of varying the dilution factor. In summary, the simulations provide strong support for the experimental results in showing that adaptation proceeds more quickly with dilution factors that are much greater than those predicted by theory to maximize the supply of surviving beneficial mutations.

Simulated Fitness Trajectories under Other Dilution Regimes. We expanded the scope of the simulations to better understand how the dilution factor affects fitness dynamics, and thereby shed more light on the limitations of the theory that is based on maximizing the supply of surviving beneficial mutations. We ran 100 replicates each for D equal to 2, 4, 8, 16, 32, 100, 300, 1000, 10^4, and 10^5, and we extended the duration of each run to 1500 transfers. Figure 7 shows the trajectories for the grand mean fitness for each dilution factor. Figure S3 provides a high-resolution picture of the grand means over the first 150 transfers, and Figure S4 shows the trajectories for the individual replicates through all 1500 transfers. These simulations reveal several noteworthy features of the evolutionary dynamics.

First, the highest final mean fitness was achieved in the 100-fold dilution regime, followed by the 32- and 300-fold dilution regimes (Fig. 7). The 16- and 1000-fold regimes were further back, followed by the 8-fold dilution regime. The 4- and 10^4-fold regimes produced yet smaller fitness gains, while the 2- and 10^5-fold dilution regimes brought up the rear. Table S9 shows that the final mean fitness values differed significantly for all pairs of adjacent regimes (e.g., $D = 100$ versus $D = 300$).

Second, analyzing the average time to divergence, *TD*, for all 10 simulated regimes yields a trend similar, but not identical, to that seen for the final fitness gains (Table S10). The 1000- and 300-fold dilutions treatments showed, on average, the fastest marker divergence, followed by the 10^4- and 100-fold dilutions. The 32- and 16-fold dilutions were next, followed by the 10^5- and 8-fold treatments, with the 4- and 2-fold dilution regimes requiring the longest times for selective sweeps to impact the ratio of the neutrally marked lineages.

Notice also that some pairs of dilution regimes showed similar fitness gains but different trajectories, especially in the early transfers. The 32- and 300-fold regimes are a striking example among the dilution factors used in our simulations. The grand mean fitness began to increase much sooner in the 300-fold regime than in the 32-fold regime, but the latter caught up by transfer 150 (Fig. S3) and kept pace through the entire 1500 transfers (Fig. 7). These varying paths introduce complications when evaluating what dilution factor promotes the greatest adaptation, because the answer may depend on the duration of the experiment.

It is also apparent that the grand mean fitness trajectories across a wide range of dilution factors are strikingly parallel after the more complex trajectories manifest during the early transfers (Fig. 7). To see this more clearly, we calculated the change in fitness over the last 500 transfers for each replicate run (Fig. S4), and we then compared the average change between adjacent regimes

(Table S11). There were no significant differences in the fitness gains over these 500 final transfers between any of the adjacent dilution regimes. In fact, the fitness gains during this terminal period were essentially identical even when the dilution factor ranged from 2-fold to 10^4-fold.

Simulations with Rate-Limiting Beneficial Mutations. Wahl et al. (4) showed that the supply of beneficial mutations that survive periodic bottlenecks is highest when $D \approx 7.4$. If these mutations limit adaptive evolution, then the same dilution factor should also maximize the rate of fitness increase. However, that dilution factor might not maximize the rate of fitness increase if beneficial mutations are common. Indeed, as Wahl et al. point out, when beneficial mutations are common, many that survive drift loss nonetheless go extinct owing to clonal interference between competing beneficial mutations (24). Therefore, the results of Wahl et al. (4) should be most relevant for predicting the rate of adaptive evolution under a strong-selection, weak-mutation regime (17, 18).

Our results, both experimental and simulated, show significantly faster adaptive evolution at higher dilutions, which implies that the supply of beneficial mutations is not limiting under the conditions we examined. To confirm that the predictions of Wahl et al. (4) are valid under a strong-selection, weak-mutation regime, we ran further simulations with the beneficial mutation rate reduced from 1.7×10^{-6} to 1.0×10^{-11} per genome, while keeping other parameters the same. With a final population size of 5×10^8 cells, these rates produce about 850 and 0.005 mutations per transfer cycle, respectively. Surviving beneficial mutations are few and far between at the lower rate. Therefore, we ran 10,000 replicates for 1500 transfers at each dilution factor in order to have enough replicates that would undergo some adaptation to allow a meaningful analysis.

Figure 8 shows the grand mean fitness trajectories for the various dilution treatments under this weak-mutation regime. The populations propagated with 8-fold dilutions achieved the highest

fitness levels, followed closely by the 16- and 4-fold regimes, with progressively smaller gains at both lower and higher dilutions (Table S12). These results thus support the predictions of Wahl et al. (4). Some of the trajectories for the grand mean fitness appear to have many steps (Fig. 8). However, these steps reflect the effects of the subset of populations with fitness gains on the grand mean; the vast majority of populations had no surviving beneficial mutations (Table S12). For the populations with fitness gains, each trajectory has only a single step-like increase, with the height of the step determined by the fitness effect of the surviving beneficial mutation (Fig. S5). Another revealing feature of the individual trajectories is reflected in the slope of the step-like increases in fitness— given similar fitness gains across different regimes, the slope is steeper when the dilution factor is higher than when it is lower (Fig. S5). This difference occurs because the higher dilution factor leads to more generations per transfer cycle, which allows a surviving beneficial mutation to sweep through the population in fewer cycles. In summary, our simulations support the results of Wahl et al. (4) when the supply of beneficial mutations limits the rate of adaptive evolution. In conjunction with our other simulations and experiments, however, it is clear that their analysis breaks down when beneficial mutations are not limiting.

Discussion

We performed experiments and simulations to understand how varying the dilution factor in serial-transfer protocols affects the dynamics of adaptation in large populations of asexual organisms. In particular, we consider the scenario in which both the final population size reached in each transfer cycle, N_f, and the total number of transfers that take place are held constant. We examined cases in which the minimum population size during the transfer bottleneck was still large, with at least hundreds of thousands of cells in our experiments and thousands of cells in our simulations. We

did so because our focus in this study is on the effects of moderate bottlenecks on the dynamics of adaptive evolution. These effects are not as well understood as those caused by extreme bottlenecks, which cause random mutations to accumulate and a concomitant loss of fitness over time (10–12).

In our experiments, we propagated 12 *E. coli* populations in each of four treatments with 2-, 8-, 100-, and 1000-fold dilutions for 150 days. These treatments produced different bottlenecks, but the final population sizes were the same because the cells reached the same resource-limited density. As a consequence, the populations in the four treatments also had different numbers of generations (i.e., doublings) during each daily transfer cycle. Our simulations included these same dilution regimes, as well as others in order to explore the effects of bottlenecks more broadly. They incorporated parameter values previously estimated from the LTEE, which used the same ancestor and environment as our experiments. The simulations allowed greater replication and avoided certain complications, most importantly ensuring that different dilution treatments did not affect anything other than the bottleneck size and number of generations between transfers.

Our experiments used two methods to assess the effect of the different dilution treatments on the rate of adaptation. First, we initiated each population from an equal mix of two clones that differ by a genetic marker—one that is selectively neutral in the conditions of our experiment, but which allows the clones to be distinguished because they make colonies of different colors when plated on an appropriate agar medium. This method let us track the relative abundance of the two clonal lineages, with the expectation that their frequencies would remain constant until a beneficial mutation swept through one or the other lineage. Our second method was to measure changes in relative fitness by competing evolved clones against the ancestral strain with the opposite marker state. Both methods support the same overarching conclusion, namely that adaptation proceeded significantly faster at the dilution factors of $D = 100$ and $D = 1000$ than at $D = 8$ (Figs. 3 and 5).

This result runs counter to the prediction that adaptation would be faster at the lower dilution factor of $D = 8$ (Fig. 1). That prediction is based on theory developed by Wahl et al. (4), which identified the dilution factor that would maximize the supply of surviving beneficial mutations.

These experiments provide compelling information about the effects of bottlenecks on the rate of adaptive evolution, but they have certain limitations, including relatively few populations. To address the limitations, we also performed numerical simulations. Using parameters estimated independently, these simulations support the same overarching conclusion that fitness improves significantly faster at both $D = 100$ and $D = 1000$ than at $D = 8$ (Fig. 6, Table S7). Taken together, our experiments and simulations demonstrate that losing a higher proportion of beneficial mutations during these more severe bottlenecks was overcome by compounding the advantage of the surviving beneficial mutations during the additional generations of population growth between successive bottlenecks.

On balance, our experiments and simulations produced similar results for the 8-, 100-, and 1000-fold dilution treatments (Figs. 5 and 6, Table S7), given the measurement errors in the former and the uncertain parameter estimates in the latter. However, there was a large discrepancy between the experiments and simulations for the 2-fold dilution treatment. Simulations predicted that fitness would begin to increase perceptibly under that regime only near the end of the 150-day duration, and then only to a slight extent (Fig. 6). In the experiments, by contrast, selective sweeps were often seen by the mid-point of the experiment (Fig. 2). Although the sweeps in the $D = 2$ treatment were seen later than in the other dilution regimes (Fig. 3), they occurred much earlier than expected from the simulations. Moreover, at the end of the experiment, the fitness gains for the bacteria that evolved in the 2-fold dilution treatment were as large as or larger than those in the other regimes, provided that their fitness was measured in the same dilution regime (Fig. 4). We showed that this

discrepancy occurred because the nature of selection in the 2-fold dilution treatment differed from the other treatments. At the higher dilutions, our experimental results were consistent with a simple scenario in which selection favored faster exponential growth, as also assumed in our simulations. By contrast, in the 2-fold dilution treatment, selection must have favored some other fitness-related trait, such as a shorter lag prior to exponential growth or the ability to use or tolerate some secreted metabolite in an environment with 50% spent medium from the prior day.

Wahl et al. (4) considered the same scenario as ours when they derived the dilution factor that maximizes the supply of beneficial mutations that survive periodic bottlenecks. They showed this supply is maximized when $D \approx 7.4$, and we confirmed their theoretical result using a different approach (Supplemental Text). If one assumes the supply of surviving beneficial mutations limits adaptation, then the same dilution factor should maximize the rate of fitness increase. In essence, this assumption implies that evolution operates under a strong-selection, weak-mutation regime (17, 18). To confirm this interpretation, we performed additional numerical simulations with the beneficial mutation rate reduced by several orders of magnitude, while keeping other parameters the same, such that surviving beneficial mutations were rare across all dilution factors. Under this regime, the simulated populations propagated with 8-fold dilutions attained the highest fitness, with gains reduced at both lower and higher dilutions (Fig. 8). This result confirms the utility of the theory of Wahl et al. for maximizing the rate of adaptation when beneficial mutations limit the rate of adaptation.

This result also raises a question: Why does the theory of Wahl et al. (4) fail to predict that higher dilution factors can accelerate adaptation under the conditions we studied? In short, this discrepancy shows that beneficial mutations are not rate-limiting for adaptation in our study. With the beneficial mutation rate estimated from the LTEE (1.7×10^{-6}) and the population size before

each dilution (5×10^8 cells), we expect ~850 new beneficial mutations in each transfer cycle in the 100-and 1000-fold dilution treatments. Most new mutations are lost during the transfers, but some survive. Also, the highly beneficial mutations that arose early in the LTEE confer fitness gains of only ~10% (28, 29), and they require hundreds of generations to sweep to fixation (3). The high rate of beneficial mutations and the long sweep times lead to competition and clonal interference among lineages with contending beneficial mutations (24). Under these circumstances, the speed with which beneficial mutations spread through a population plays a critical role in determining the rate of adaptive evolution. A higher dilution factor leads directly to more generations in every transfer cycle and therefore, for the same relative fitness advantage, allows a beneficial mutation to spread more quickly. This effect can be seen even in the weak-mutation regime, where surviving mutations that confer similar benefits sweep more quickly at higher dilution factors (Fig. S5). The faster spread has a negligible effect when the supply of beneficial mutations limits the rate of adaptation, but it is important when beneficial mutations are plentiful.

In short, the analysis of Wahl et al. (4) reflects the effect of selection on the probability that beneficial mutations survive periodic bottlenecks, and it accurately predicts the dilution factor that maximizes adaptation when beneficial mutations are limiting. However, it does not account for the number of generations between periodic bottlenecks, which depends on the dilution factor, and which determines the speed with which surviving beneficial mutations spread through a population. Changing the dilution factor therefore has two opposing effects (Fig. 1). On the one hand, greater dilutions cause more severe bottlenecks, leading to the stochastic loss of more beneficial mutations soon after they arise. On the other hand, greater dilutions also allow more generations of growth in each transfer cycle, so that the fitness advantages of surviving beneficial mutations compound at a faster rate.

Future Directions. Our results show that the effects of periodic bottlenecks on the dynamics of adaptation involve an interplay between the loss of beneficial mutations and the rate of spread of surviving beneficial mutants. However, a number of interesting questions remain for future work. In terms of our experiments, it would be interesting to understand why the effects of selection were so different in the 2-fold dilution treatment from the other treatments. With 8-, 100-, and 1000-fold dilutions, our results were consistent with simple selection for faster growth. In the 2-fold regime, selection appears to have favored other fitness components. For example, the bacteria might have evolved a shorter lag before starting growth after each transfer (15); or they might tolerate and even exploit secreted metabolites from the previous day (30), which could be especially important in their half-spent medium. Whole-genome sequencing of the evolved bacteria might show where and how the genetic targets of selection differ between the 2-fold and other dilution treatments (31), which could provide insights into the phenotypic traits under selection.

In terms of theory, numerical simulations can guide future efforts to identify the dilution factor that maximizes adaptation under conditions more general than those considered by Wahl et al. (4). Simulations as well as more general theory would enable one to examine the sensitivity of the optimal dilution factor and the resulting rate of adaptation to other parameters in the model. It should be kept in mind, however, that the rate of adaptation is not static; rather, it accelerates as early beneficial mutations begin to sweep, and later decelerates owing to diminishing-returns epistasis (13, 24). Therefore, it is quite possible that the optimum dilution factor changes over time.

Another set of questions concerns the interplay of beneficial and deleterious mutations. In our simulations, we ignored deleterious mutations. We did so because the mutation rate in *E. coli* cells with functional DNA repair is extremely low. From the rate of accumulation of synonymous mutations in the LTEE, the point-mutation rate has been estimated as $\sim 10^{-10}$ per bp per generation

(16). With a genome length of ~5×10^6 bp, this rate implies fewer than 0.001 mutations per genome replication, and many of them will be neutral rather than deleterious. The rates of other types of mutations, including insertions and deletions, are less certain, but mutation-accumulation experiments indicate that the genome-wide rate of all deleterious mutations is very low (10, 12). However, some of the LTEE lines evolved hypermutability that increased their point-mutation rates by ~100-fold (12, 14, 32). Moreover, as the LTEE goes forward, the rate of adaptive evolution should continue to slow owing to the prevalence of diminishing-returns epistasis (13). As a consequence of increased mutation rates, reduced effect-sizes of beneficial mutations, or both, deleterious mutations may eventually become relevant for understanding the dynamics of adaptive evolution in the LTEE. More generally, deleterious mutations are important in some other microbial evolution experiments, such as with highly mutable RNA viruses or when imposing more severe bottlenecks that allow some deleterious mutations to fix. Therefore, it will be interesting to perform simulations and develop theory that examines the combined effects of deleterious and beneficial mutations on the dynamics of adaptive evolution in populations subject to periodic bottlenecks.

Materials and Methods

Evolution Experiment and Dilution Regimes. We isolated 12 clones as single colonies from freezer stocks of each of two *E. coli* strains, REL606 (Ara^-) and REL607 (Ara^+). The clones were incubated in Luria-Bertani broth for 24 h, then diluted 10,000-fold into Davis minimal medium supplemented with 25 μg/mL glucose (DM25) and incubated for another 24 h. On day 0 of the evolution experiment, we mixed one Ara^- isolate and one Ara^+ isolate equally to make 12 mixed cultures. These cultures were transferred to test-tubes containing fresh DM25 medium using four different dilution regimes. For the 2-fold treatment, we transferred 5 mL of each mixed culture into

5 mL of DM25. For the 8-fold treatment, we transferred 1.25 mL of each culture into 8.75 mL of DM25. For the 100-fold treatment, we transferred 0.1 mL into 9.9 mL of DM25. For the 1000-fold treatment, we diluted a portion of each mixed culture 10-fold in saline solution and then transferred 0.1 mL into 9.9 mL of DM25. By using the same culture volume and resource concentration, the bacteria should reach the same final population size in all four treatments. However, the number of generations (doublings) varies with the treatment, such that the bacteria undergo 1, 3, ~6.6, or ~10 generations per daily transfer cycle. We incubated the 48 populations for 24 h and transferred them daily following the same dilution protocols for 150 days. All cultures were kept at 37 ºC. Every 15 days, we froze samples of each population at –80 ºC with glycerol as a cryoprotectant.

Marker Divergence Analysis. During the evolution experiment, we diluted and spread cells from each population on tetrazolium arabinose (TA) indicator agar plates on days 0, 1, 3, and every 3 days thereafter for the first 90 days to track the ratio of the Ara^- and Ara^+ lineages. Most of the populations in the 1000-fold dilution treatment had fixed one of the marker states by day 90, and we subsequently plated them only every 15 days. Similarly, we plated the populations in the 100-fold treatment every 15 days from day 120 onward.

Fitness Measurements. We isolated clones from each population after 90 and 150 transfers (Table S13). The clones isolated after 150 transfers were taken from the numerically dominant marked lineage at that point. We used clones sampled after 90 transfers from the same marked lineage to avoid confusion while performing competition assays; in most cases, the same lineage was dominant at both time points. These clones competed against the ancestral strain with the opposite marker state, which allowed us to enumerate them by plating on TA agar. Our methods were the same as described elsewhere for the LTEE (3, 13, 33) except in three respects: (i) the competitions were performed in test-tubes, rather than in flasks; (ii) the volume of the inoculum and the dilution factor varied, as indicated for the reported assays; and (iii) the competitions ran for multiple days, with daily dilutions, to estimate small fitness differences with greater precision. In particular, we ran competitions under the 2-fold dilution regime for 12 days (12 generations),

the 8-fold regime for 6 days (18 generations), and the 100-fold and 1000-fold regimes for 2 days (~13.3 and ~20 generations, respectively). Relative fitness is calculated as the ratio of the realized growth rate of the evolved competitor to that of its ancestral counterpart during the competition assay: $W = \ln (D^n \times E_f / E_i) / \ln (D^n \times A_f / A_i)$, where D is the dilution factor, n is the number of transfers (i.e., the duration of the assay minus 1), E_i and E_f are the initial and final densities of the evolved competitor, and A_i and A_f are the corresponding densities of the ancestor.

Computer Simulations. We wrote a program called STEPS—for Serially Transferred Evolving Populations Simulation—to simulate fitness and marker trajectories. The program tracks unique lineages, each defined by one or more mutations, in a population propagated by serial transfers. Each population starts with an initial size of N_f / D, where N_f is the final population size and D is the dilution factor. Each population begins with two equally abundant lineages that differ only by a neutral marker. Beneficial mutations are introduced at random as the population grows, thereby generating new lineages that are tracked over time. The lineages grow exponentially according to their relative fitness values. Growth continues until the total population reaches its final size. At that point, its mean fitness is recorded along with the ratio of the two markers. The population is then bottlenecked according to the specified dilution factor, with survivors determined by randomly sampling the lineages. Except as otherwise stated, all of the simulations in this study used the following inputs: final population size, $N_f = 5 \times 10^8$; beneficial mutation rate, $\mu_B = 1.7 \times 10^{-6}$; mean effect size of beneficial mutations in the ancestor, $s = 0.01587$; and strength of diminishing-returns epistasis, $g = 6.0217$. The first value corresponds to the ancestor's final population size in the LTEE (3); the other three values were estimated from the fitness dynamics during the first 50,000 generations of the LTEE (13). We provide further details regarding implementation of the simulations in the Supplemental Text.

Statistical Analyses. Analyses were performed using the referenced tests in R version 4.1.2.

ACKNOWLEDGMENTS. We thank Chitrak Banerjee, Michael Desai, Ben Good, Thomas LaBar, Charles Ofria, and Mike Wiser for valuable discussions, and Neerja Hajela and Jessica Baxter for assistance in the lab. We acknowledge funding from the Yamada Science Foundation (to MI), the Japan Society for the Promotion of Science (to MI), the MSU Professorial Assistants Program (to JPD), the National Science Foundation (DEB-1951307 to REL), the USDA National Institute of Food and Agriculture (MICL02253 to REL), and the BEACON Center for the Study of Evolution in Action (NSF Cooperative Agreement DBI-0939454).

References

1. M. Kimura, T. Ohta, Probability of gene fixation in an expanding finite population. *Proc. Natl. Acad. Sci. U.S.A.* **71**, 3377–3379 (1974).
2. S. P. Otto, M. C. Whitlock, The probability of fixation in populations of changing size. *Genetics* **146**, 723–733 (1997).
3. R. E. Lenski, M. R. Rose, S. C. Simpson, S. C. Tadler, Long-term experimental evolution in *Escherichia coli*. I. Adaptation and divergence during 2,000 generations. *Am. Nat.* **138**, 1315–1341 (1991).
4. L. M. Wahl, P. J. Gerrish, I. Saika-Voivod, Evaluating the impact of population bottlenecks in experimental evolution. *Genetics* **162**, 961–971 (2002).
5. J. E. Barrick, R. E. Lenski, Genome dynamics during experimental evolution. *Nat. Rev. Genet.* **14**, 827–839 (2013).
6. S. F. Elena, R. Sanjuán, A. V. Bordería, P. E. Turner, Transmission bottlenecks and the evolution of fitness in rapidly evolving RNA viruses. *Infect. Genet. Evol.* **1**, 41–48 (2001).
7. A. Abel, P. Abel zur Wiesch, B. M. Davis, M. K. Waldor, Analysis of bottlenecks in experimental models of infection. *PLoS Pathog.* **11**, e1004823 (2015).

8. R. Moxon, E. Kussell, The impact of bottlenecks on microbial survival, adaptation, and phenotypic switching in host–pathogen interactions. *Evolution* **71**, 2803–2816 (2017).
9. A. Sousa *et al.,* Recurrent reverse evolution maintains polymorphism after strong bottlenecks in commensal gut bacteria. *Mol. Biol. Evol.* **34**, 2879–2892 (2017).
10. T. T. Kibota, M. Lynch, Estimate of the genomic mutation rate deleterious to overall fitness in *E. coli*. *Nature* **381**, 694–696 (1996).
11. A. Caballero, E. Cusi, C. Garcia, A. García-Dorado, Accumulation of deleterious mutations: additional *Drosophila melanogaster* estimates and a simulation of the effects of selection. *Evolution* **56**, 1150–1159 (2002).
12. O. Tenaillon *et al*., Tempo and mode of genome evolution in a 50,000-generation experiment. *Nature* **536**, 165–170 (2016).
13. M. J. Wiser, N. Ribeck, R. E. Lenski, Long-term dynamics of adaptation in asexual populations. *Science* **342**, 1364–1367 (2013).
14. B. H. Good *et al*., The dynamics of molecular evolution over 60,000 generations. *Nature* **551**, 45–50 (2017).
15. F. Vasi, M. Travisano, R. E. Lenski, Long-term experimental evolution in *Escherichia coli*. II. Changes in life-history traits during adaptation to a seasonal environment. *Am. Nat.* **144**, 432–456 (1994).
16. S. Wielgoss *et al*., Mutation rate inferred from synonymous substitutions in a long-term evolution experiment with *Escherichia coli*. *G3 (Bethesda)* **1**, 183–186 (2011).
17. J. H. Gillespie, *The Causes of Molecular Evolution* (Oxford University Press, 1991).
18. P. D. Sniegowski, P. J. Gerrish, Beneficial mutations and the dynamics of adaptation in asexual populations. *Phil. Trans. R. Soc. B.* **365**, 1255–1263 (2010).
19. Y. D. Chavhan, S. I. Ali, S. Dey, Larger numbers can impede adaptation in asexual populations despite entailing greater genetic variation. *Evol. Biol.* **46**, 1–13 (2019).

20. T. Wein, T. Dagan, The effect of population bottleneck size and selective regime on genetic diversity and evolvability in bacteria. *Genome Biol. Evol.* **11**, 3283–3290 (2019).
21. L. Garoff *et al*., Population bottlenecks strongly influence the evolutionary trajectory to fluoroquinolone resistance in *Escherichia coli*. *Mol. Biol. Evol.* **37**, 1637–1646 (2020).
22. Y. D. Chavhan, S. Malusare, S. Dey, Interplay of population size and environmental fluctuations: A new explanation for fitness cost rarity in asexuals. *Ecology Letters* **24**, 1943–1954 (2021).
23. N. Mahrt *et al*., Bottleneck size and selection level reproducibly impact evolution of antibiotic resistance. *Nat. Ecol. Evol.* **5**, 1233–1242 (2021).
24. P. J. Gerrish, R. E. Lenski, The fate of competing beneficial mutations in an asexual population. *Genetica* **102**, 127–144 (1998).
25. J. E. Barrick, M. R. Kauth, C. C. Strelioff, R. E. Lenski, *Escherichia coli rpoB* mutants have increased evolvability in proportion to their fitness defects. *Mol. Biol. Evol.* **27**, 1338–1347 (2010).
26. S. F. Levy *et al.*, Quantitative evolutionary dynamics using high-resolution lineage tracking. *Nature* **519**, 181–186 (2015).
27. R. E. Lenski *et al.*, Sustained fitness gains and variability in fitness trajectories in the long-term evolution experiment with *Escherichia coli*. *Proc. R. Soc. B* **282**, 20152292 (2015).
28. J. E. Barrick *et al*., Genome evolution and adaptation in a long-term experiment with *Escherichia coli*. *Nature* **461**, 1243–1247 (2009).
29. A. I. Khan, D. M. Dinh, D. Schneider, R. E. Lenski, T. F. Cooper, Negative epistasis between beneficial mutations in an evolving bacterial population. *Science* **332**, 1193–1196 (2011).
30. T. Großkopf *et al*., Metabolic modelling in a dynamic evolutionary framework predicts adaptive diversification of bacteria in a long-term evolution experiment. *BMC Evol. Biol.* **16**, 163 (2016).

31. D. E. Deatherage, J. L. Kepner, A. F. Bennett, R. E. Lenski, J. E. Barrick, Specificity of genome evolution in experimental populations of *Escherichia coli* evolved at different temperatures. *Proc. Natl. Acad. Sci. U.S.A.* **114**, E1904–E1912 (2017).
32. P. D. Sniegowski, P. J. Gerrish, R. E. Lenski, Evolution of high mutation rates in experimental populations of *Escherichia coli. Nature* **387**, 703–705 (1997).
33. R. E. Lenski, M. Travisano, Dynamics of adaptation and diversification: a 10,000-generation experiment with bacterial populations. *Proc. Natl. Acad. Sci. U.S.A.* **91**, 6808–6814 (1994).

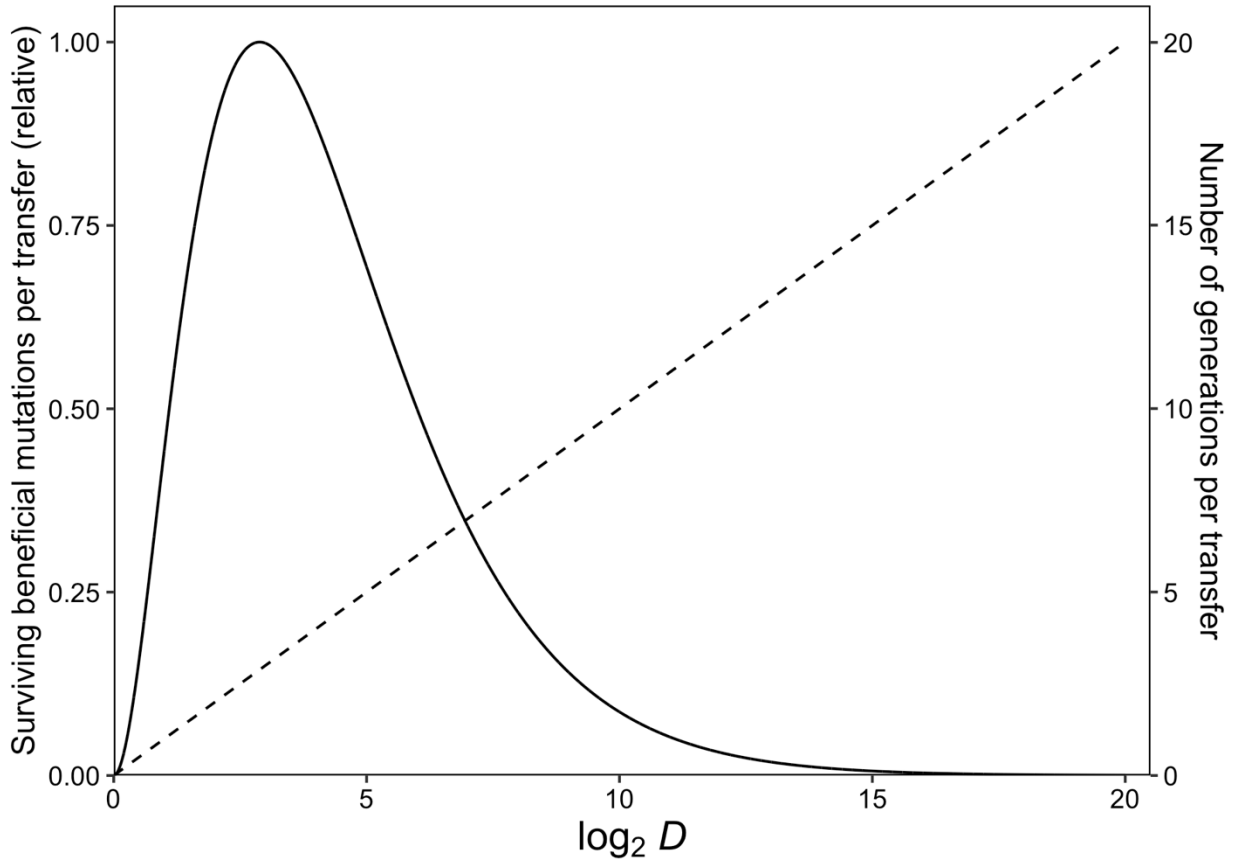

Fig. 1. Effects of varying the dilution factor, *D*, in asexual populations propagated via periodic serial transfers. Solid curve shows the effect on the number of surviving beneficial mutations per transfer (left scale). Dashed line shows the effect on the number of generations of growth between successive transfer events (right scale). Note the $\log_2$-transformed scale for *D*.

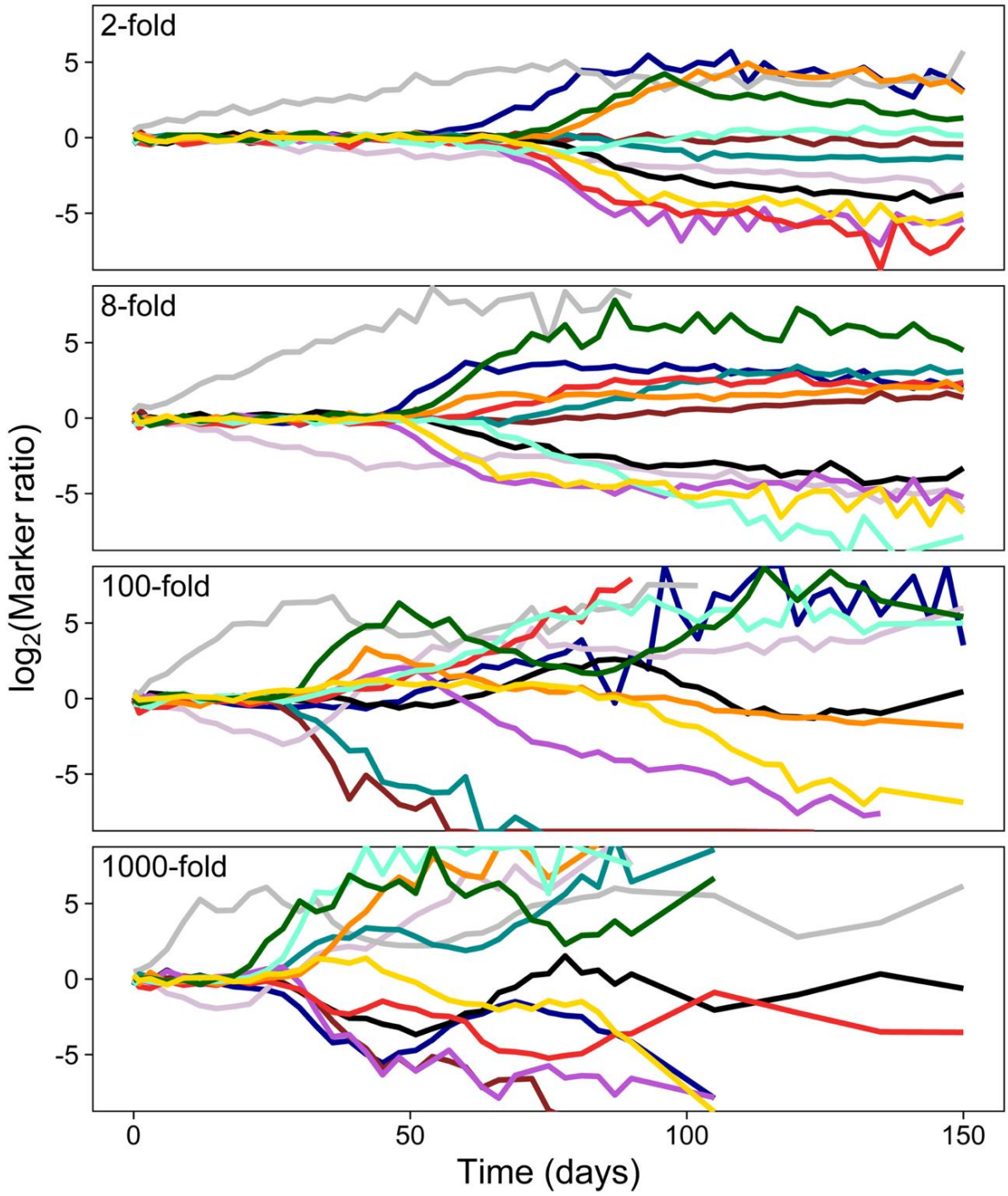

Fig. 2. Trajectories of the relative abundance of two marked lineages in 12 *E. coli* populations evolving in each of 4 dilution regimes for 150 daily transfers. With a neutral marker, the ratio remains essentially constant until a beneficial mutation begins to sweep through one of the lineages. Two populations (gray and mauve lines) in each regime were founded by the same pair of clones that had non-neutral mutations, and they were excluded from the analysis of time to divergence of the marker ratio. Note the $\log_2$-transformed scale for the marker ratio.

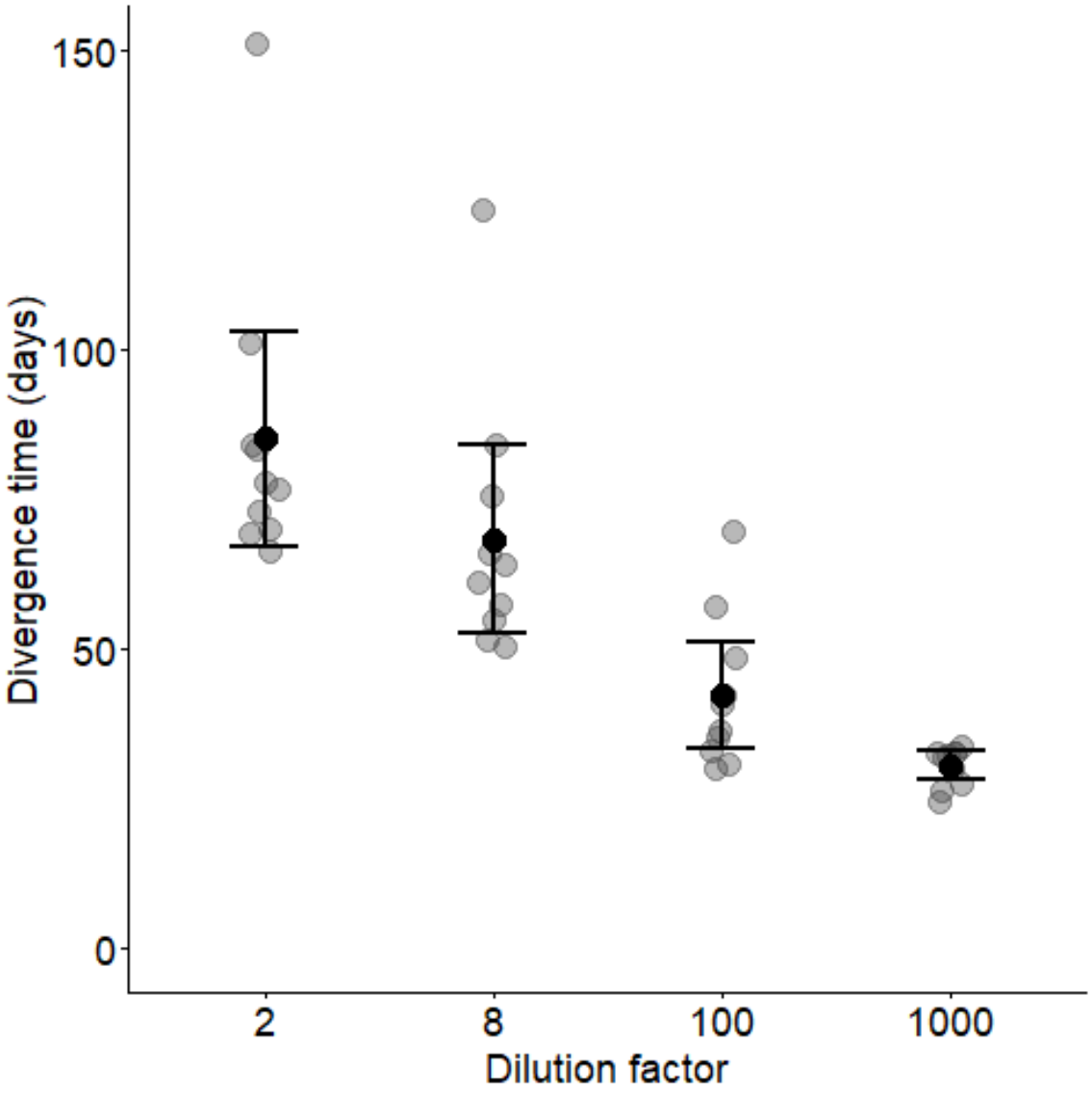

Fig. 3. Time to divergence, *TD*, of the marker ratio in populations propagated under different dilution regimes. For each population, *TD* is defined as the first sample when the ratio of the neutrally marked lineages deviated from unity by two-fold in either direction, based on counts made every third day. Black and gray symbols show means and replicate assays, respectively; error bars are 95% confidence intervals. See text for details and Table S2 for statistical analysis.

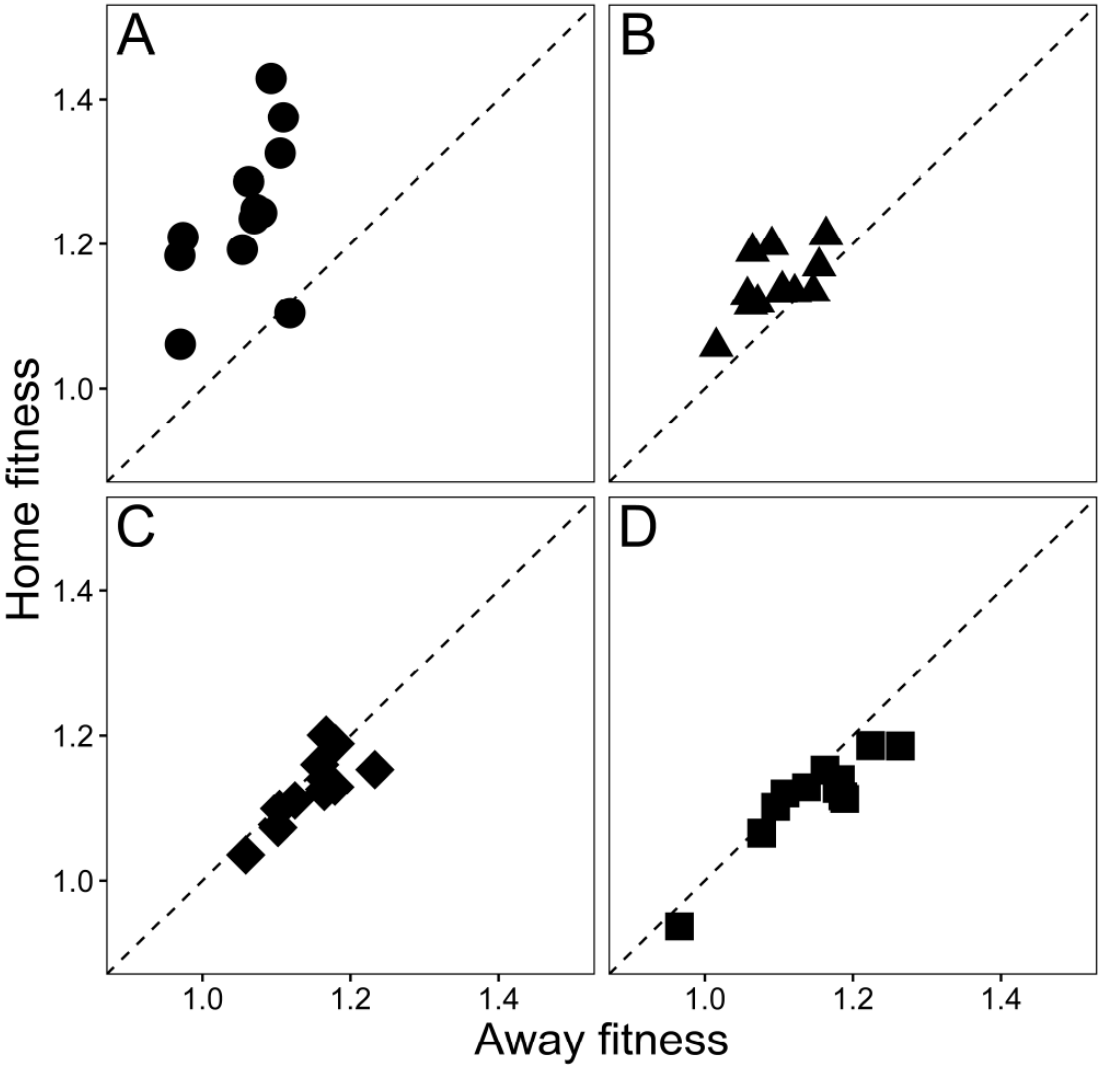

Fig. 4. Comparisons of fitness measured in "home" and "away" environments for bacteria that evolved with 2-fold (A), 8-fold (B), 100-fold (C), and 1000-fold (D) daily dilutions for 150 days. In the home environment, the evolved bacteria competed against a marked ancestor under the same dilution regime where they had evolved. In the away environment, all of the competition assays used 100-fold daily dilutions, regardless of the evolutionary regime. The dashed lines show the expectation if fitness values are equal in the two environments.

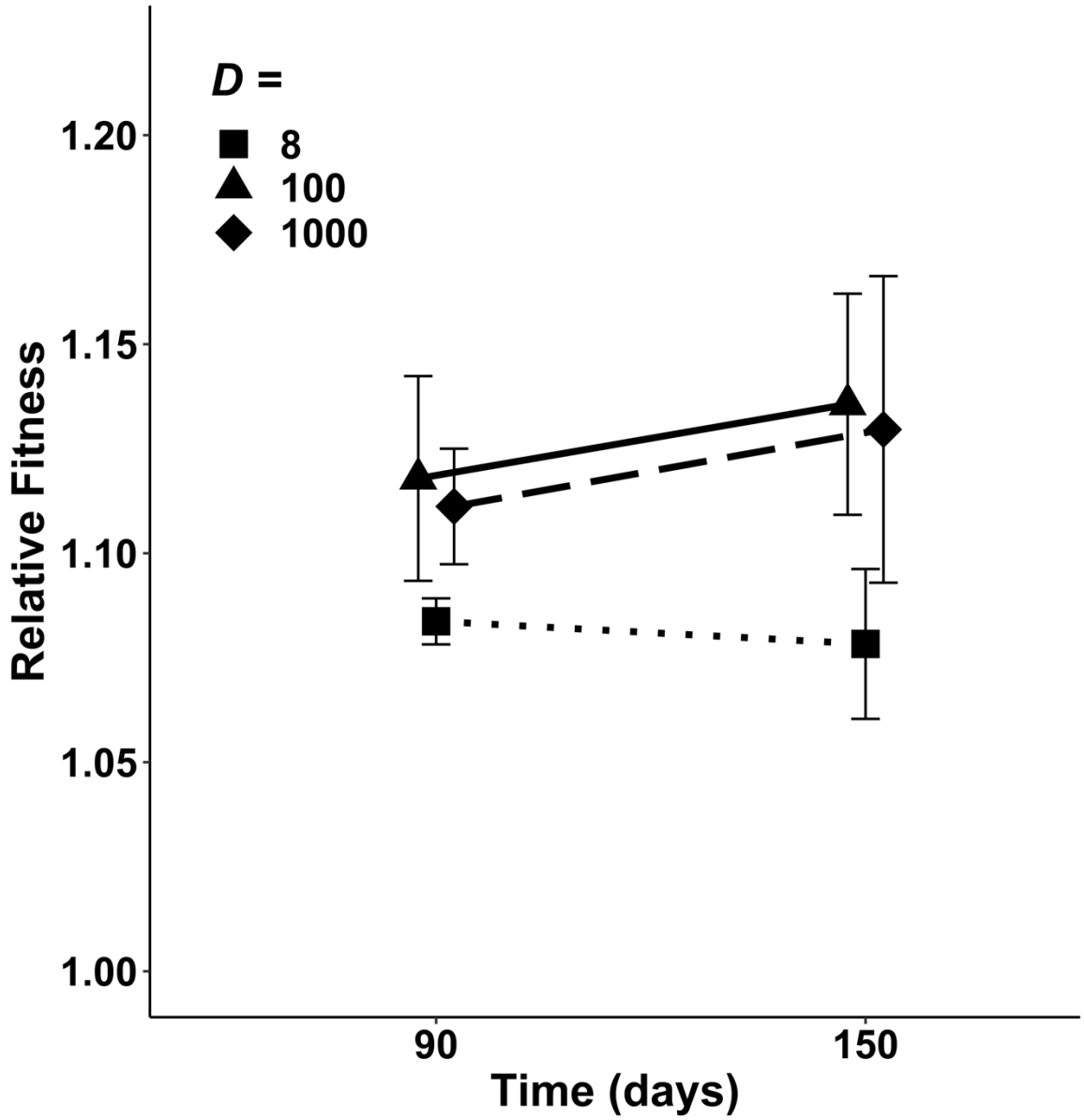

Fig. 5. Change in relative fitness between days 90 and 150 for bacteria that evolved with 8-fold, 100-fold, and 1000-fold daily dilutions. Error bars show 95% confidence intervals based on the replicate populations in each treatment.

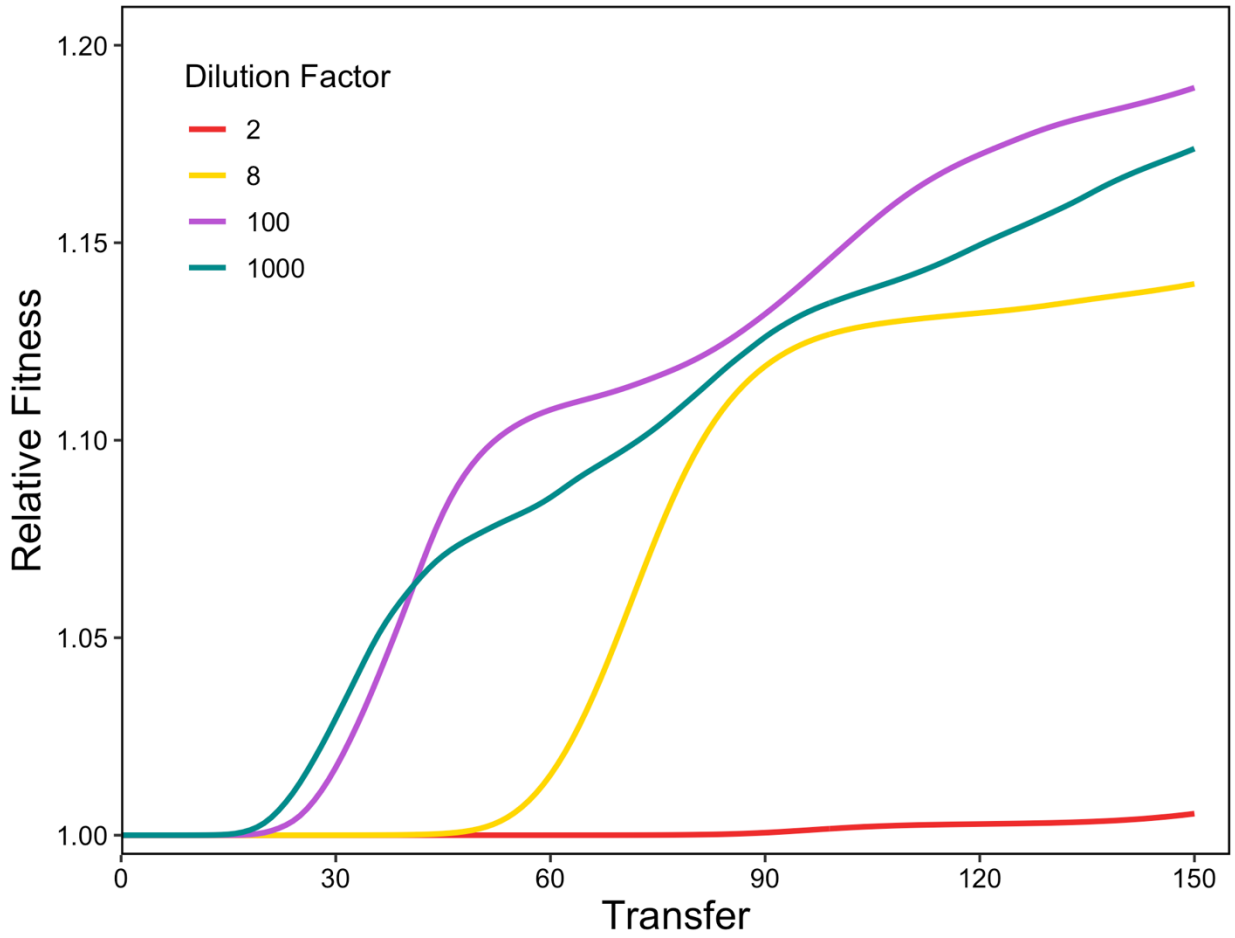

Fig. 6. Simulated trajectories of relative fitness for populations evolving with 2-fold, 8-fold, 100-fold, and 1000-fold dilutions. Each trajectory shows the grand mean fitness based on 100 runs for 150 transfer events. See text for details.

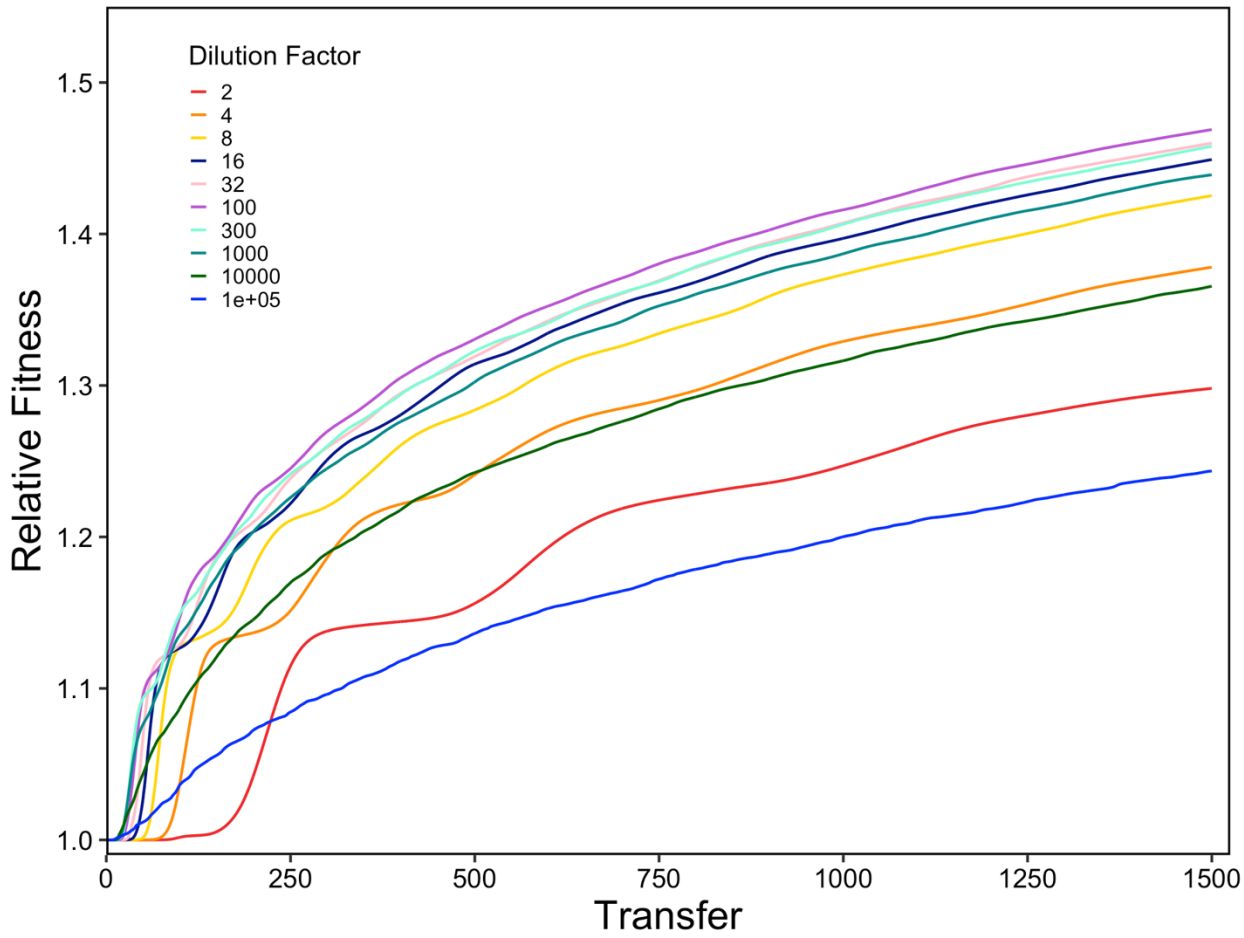

Fig. 7. Extended simulations showing trajectories of relative fitness for populations evolving with dilution factors ranging from 2-fold to 10^5-fold. Each trajectory shows the grand mean fitness based on 100 runs for 1500 transfer events. Individual runs are shown in Fig. S4.

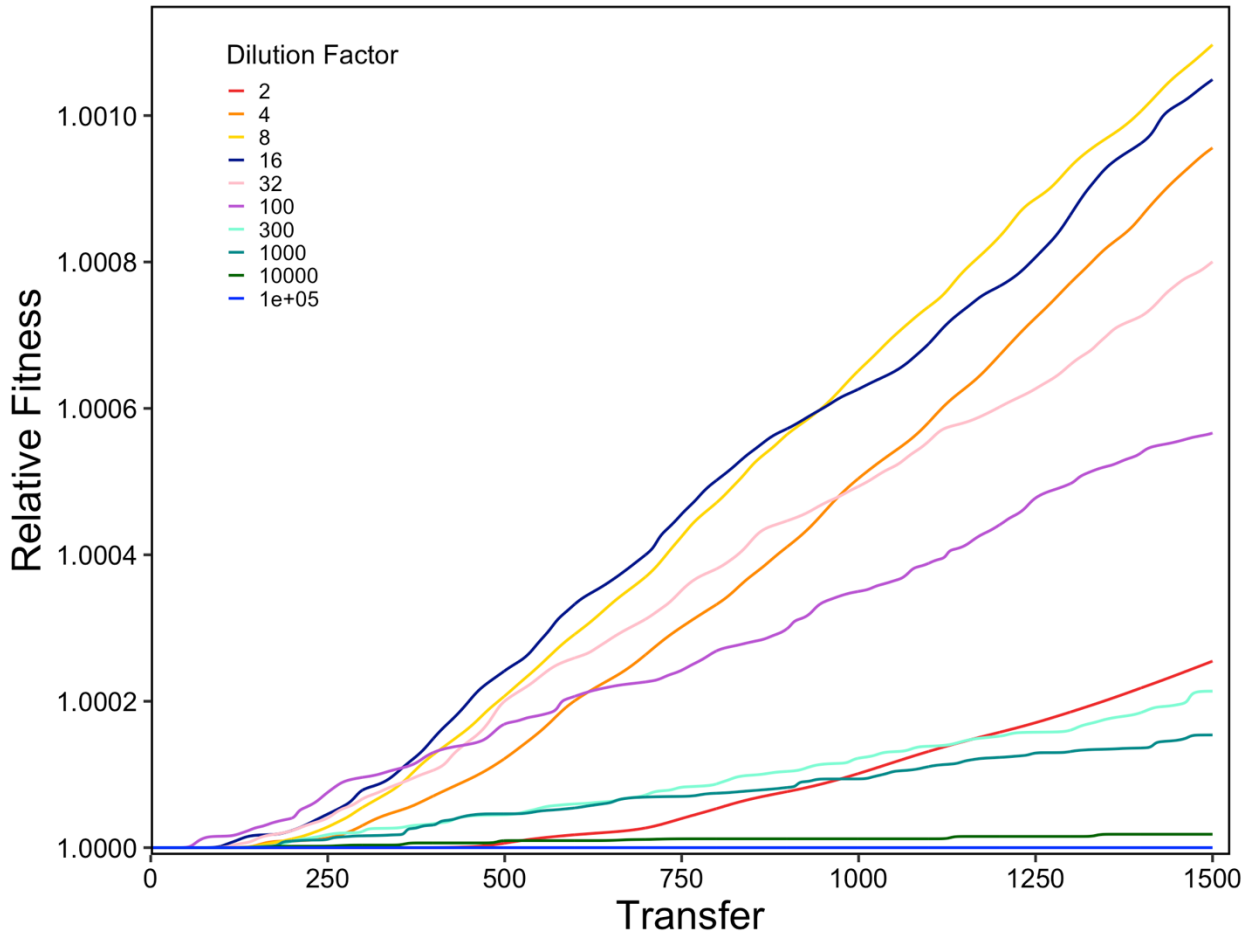

Fig. 8. Simulations showing trajectories of relative fitness for populations evolving under a mutation-limited regime with dilution factors ranging from 2-fold to 10^5-fold. Each trajectory shows the grand mean fitness based on 10,000 runs for 1500 transfer events. Individual runs are shown in Fig. S5. See text for details.

Supplementary Information for

Effects of periodic bottlenecks on the dynamics of adaptive evolution in microbial populations

Minako Izutsu, Devin M. Lake, Zachary W. D. Matson, Jack P. Dodson, and Richard E. Lenski

Corresponding authors: Minako Izutsu and Richard E. Lenski

Email: izutsumi@msu.edu and lenski@msu.edu

This PDF file includes:

Supplementary text
Figures S1 to S5
Tables S1 to S13
SI References

Supplementary Information Text

Alternative derivation of the supply of beneficial mutations that survive drift loss. Here we present a simple derivation of the dilution factor, D, that maximizes the number of beneficial mutations that survive drift loss in an evolution experiment with periodic serial transfers. Let beneficial mutations occur at the rate μ_B. We assume the mutations have small to moderate effects (usually less than ~10%), as they do in our experiments and simulations. We assume that the rate of deleterious mutations is low enough that they have no effect on the survival of beneficial mutations. We also assume that there is enough time between transfers for the cells to reach the same final population size, N_f, in each transfer cycle, regardless of the dilution factor, and that no cell death occurs after reaching that final size. In addition, we assume that genotypes differ only in their growth rate, and not in any other demographic parameter. We further assume that experiments run for the same number of transfers, regardless of the dilution factor. As a consequence, the total number of generations, G_{tot}, during an experiment depends on the dilution factor, increasing as $G_{tot} = T \log_2 D$, where T is the number of transfers and generations are expressed as cell doublings.

Given repeated bottlenecks, the effective population size with respective to the probability of survival of beneficial mutations, N_e, is approximated by $G\ N_{min}$, where $N_{min} = N_f / D$ is the bottlenecked population size and $G = \log_2 D$ is the number of generations for the population size to increase from N_{min} to N_f (1–3). We now want to maximize the cumulative number of surviving beneficial mutations, M, across T transfer cycles, where each cycle involves G generations with an effective population size, N_e:

$$M = \mu_B\ G\ N_e\ T$$

$$= \mu_B\ G^2\ N_f\ T / 2^G.$$

Taking the first derivative of M with respect to G, we obtain:

$$\mathrm{d}M / \mathrm{d}G = -\mu_B\ G\ N_f\ T\ (G \ln 2 - 2) / 2^G.$$

This derivative has a unique positive root $G = 2 / \ln 2 \approx 2.89$. The corresponding value of the dilution factor that maximizes the cumulative number of beneficial mutations that survive drift loss is then $D = 2^G = e^2 \approx 7.39$. Our solution agrees precisely with the solution obtained by Wahl *et al.* (3).

This solution addresses the production of beneficial mutations and the probability that they are not lost to random drift while they are still rare. It does not, however, account for differences in growth rate (relative fitness) among surviving beneficial mutations that determine the speed with which they increase in relative abundance. A larger dilution factor, D, necessarily leads to more generations, G, over the same number of transfers, T. More generations, in turn, will amplify the differences in growth rate. Consequently, optimizing the supply of surviving beneficial mutations is insufficient to predict the dilution factor that maximizes the rate of improvement in fitness, except when beneficial mutations are so rare that they are rate-limiting. In general, the optimal dilution factor for maximizing the rate of fitness gain should be greater than the value of D derived above, as we see in our experiments and simulations, and as dictated by the logic of compounding.

Methods

Computer simulations. We wrote and implemented the STEPS program to simulate the trajectories for relative fitness and marker ratios in populations undergoing periodic serial transfers (https://github.com/zachmatson/STEPS/releases/tag/v1.0.0). Each run tracks a population of clonal lineages as they grow and mutate; the population then undergoes a bottleneck when it reaches the final size, N_f. For each lineage, the program tracks its fitness, number of individuals, neutral marker state, and parent lineage, and all these data are saved after every transfer. From these data, we can compute the trajectories of the marker ratio and mean fitness as well as track the mutation dynamics.

For the growth phase between transfers, we simulate a fixed number of timesteps based on the dilution factor, D. During each step, the growth rate of a lineage is determined by its fitness. The number of timesteps is such that the total population size approximately doubles in each step, except for the final step. The program calculates the duration of the timesteps at the start of every growth phase, such that the length of each step (except for the last one) is scaled inversely to the population mean fitness. This scaling allows the lineages with above-average fitness to more than double during that step, while lineages with below-average fitness increase less than two-fold. The last timestep in each transfer cycle is done differently, such that the total population grows only enough to reach the fixed final size (rather than double).

Mutations enter the population during each timestep. The expected number of mutations equals the product of the beneficial mutation rate, μ_B, and number of individuals produced in that step, with sampling from a Poisson distribution (4). The mutations are randomly distributed among lineages, with the expected numbers proportional to their relative abundances. Each mutation creates a new lineage with fitness W_{new}. Following the model of Wiser *et al.* (5), $W_{new} = W(1 + s)$, where W is the fitness of the parent genotype relative to the ancestor, and s is the effect size of the new mutation. The fitness effects are drawn from an exponential distribution, $\alpha e^{-\alpha s}$, that depends on the parent genotype's fitness, as follows: $\alpha_{n+1} = \alpha_n (1 + g\, s_{n+1})$, where $s_0 = 1/\alpha_0$ is the mean of the initial distribution, s_{n+1} is the effect size of the n+1 mutation, and g governs the strength of diminishing-returns epistasis. Note that Wiser *et al.* reported $\alpha_0 = 85$ (such that $s_0 = 0.01176$), whereas we use $\alpha_0 = 63$ (such that $s_0 = 0.01587$); this difference reflects the implementation of population growth on $\log_e$ and $\log_2$ scales, respectively.

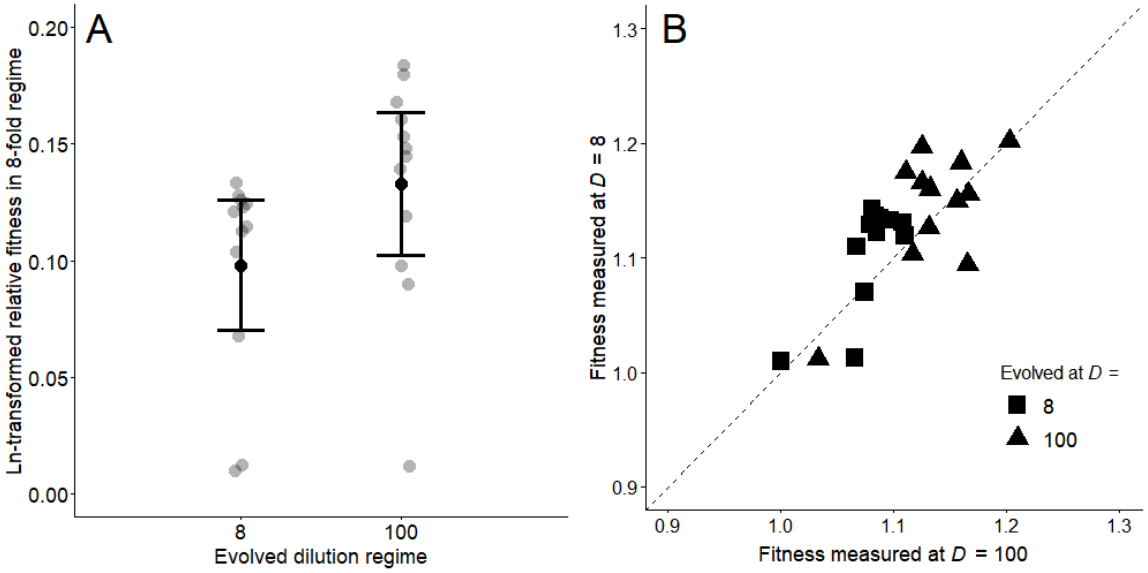

Fig. S1. Bacteria that evolved in the 100-fold dilution regime were more fit than those that evolved in the 8-fold regime, regardless of the competition environment. (A) Comparison of ln-transformed fitness values for bacteria that evolved in these two regimes, when both sets competed against marked ancestors in the 8-fold regime. Black and gray symbols show means and replicate assays, respectively, and error bars are 95% confidence intervals. The bacteria that evolved with 100-fold dilutions were more fit than those that evolved with 8-fold dilutions, even in the 8-fold regime (p = 0.0342, two-tailed Wilcoxon's signed-ranks test). (B) Correlation of fitness values measured in the 8-fold and 100-fold dilution regimes for bacteria that evolved in those two regimes. The overall correlation was strong and highly significant (r = 0.7399, p < 0.0001).

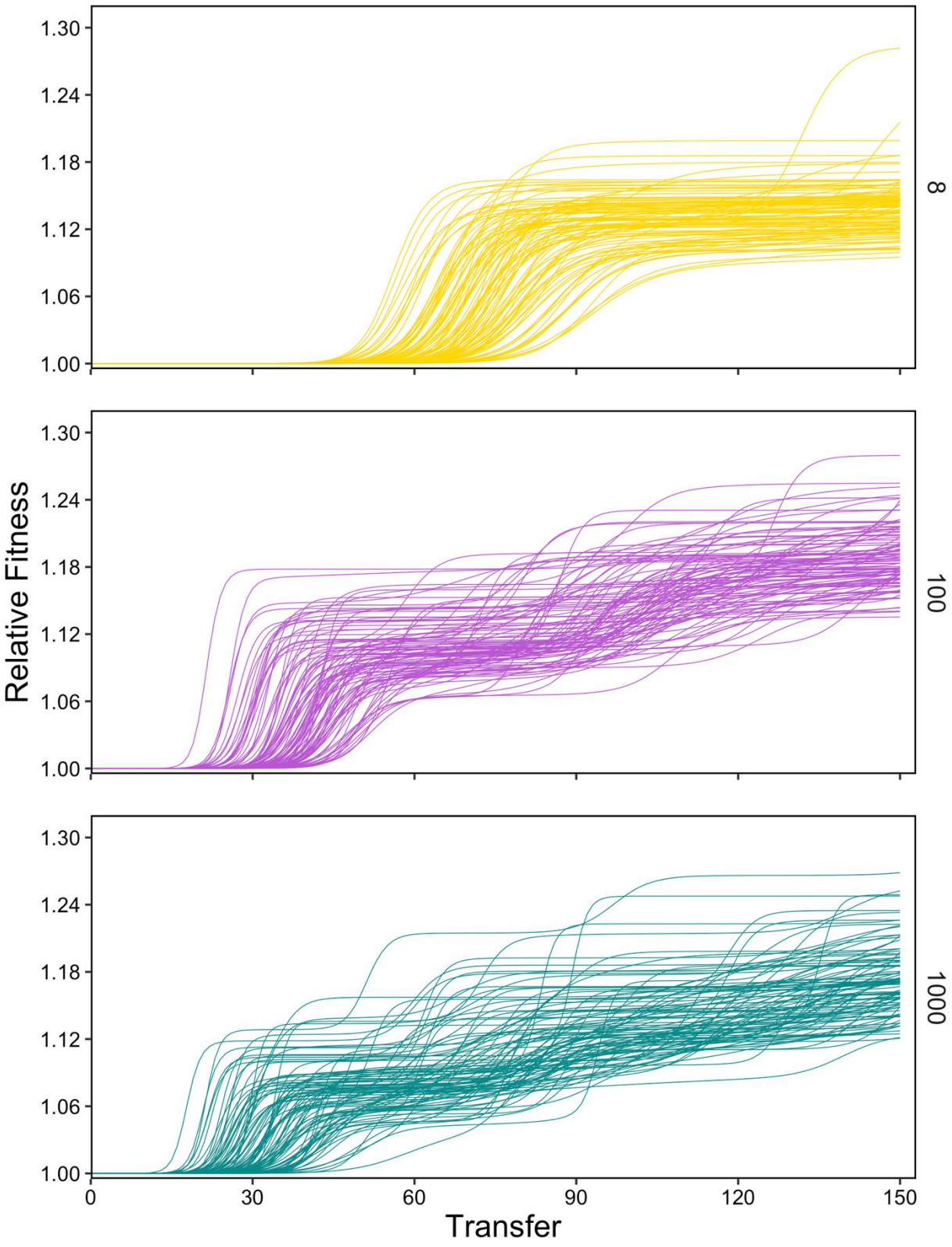

Fig. S2. Simulated relative-fitness trajectories for 100 populations evolving with 8-fold, 100-fold, and 1000-fold dilutions for 150 transfers. Trajectories for the grand means are shown in Fig. 6.

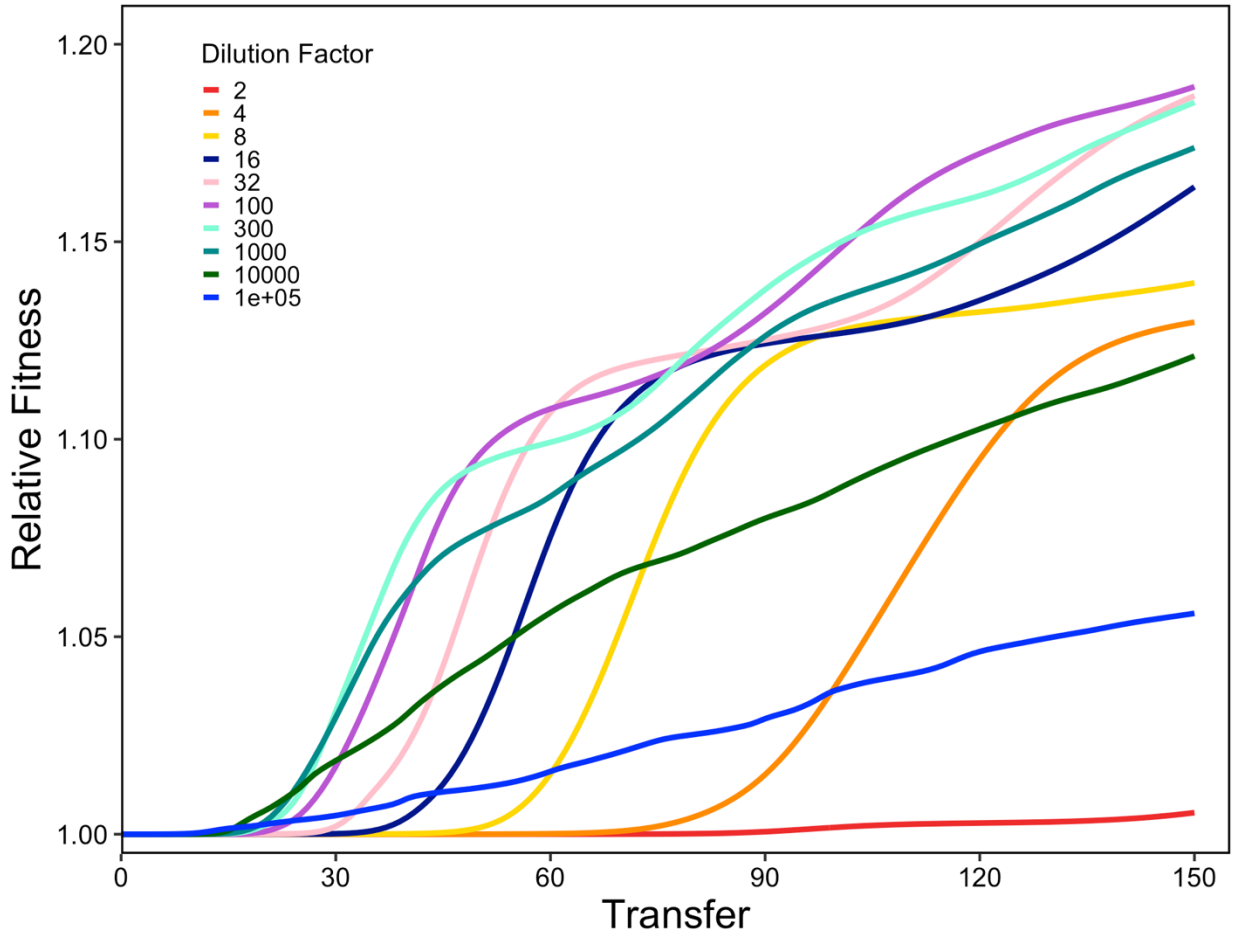

Fig. S3. Extended simulations showing trajectories of relative fitness for populations evolving with dilution factors ranging from 2-fold to 10^5-fold. Each trajectory shows the grand mean of 100 runs for the first 150 transfers only.

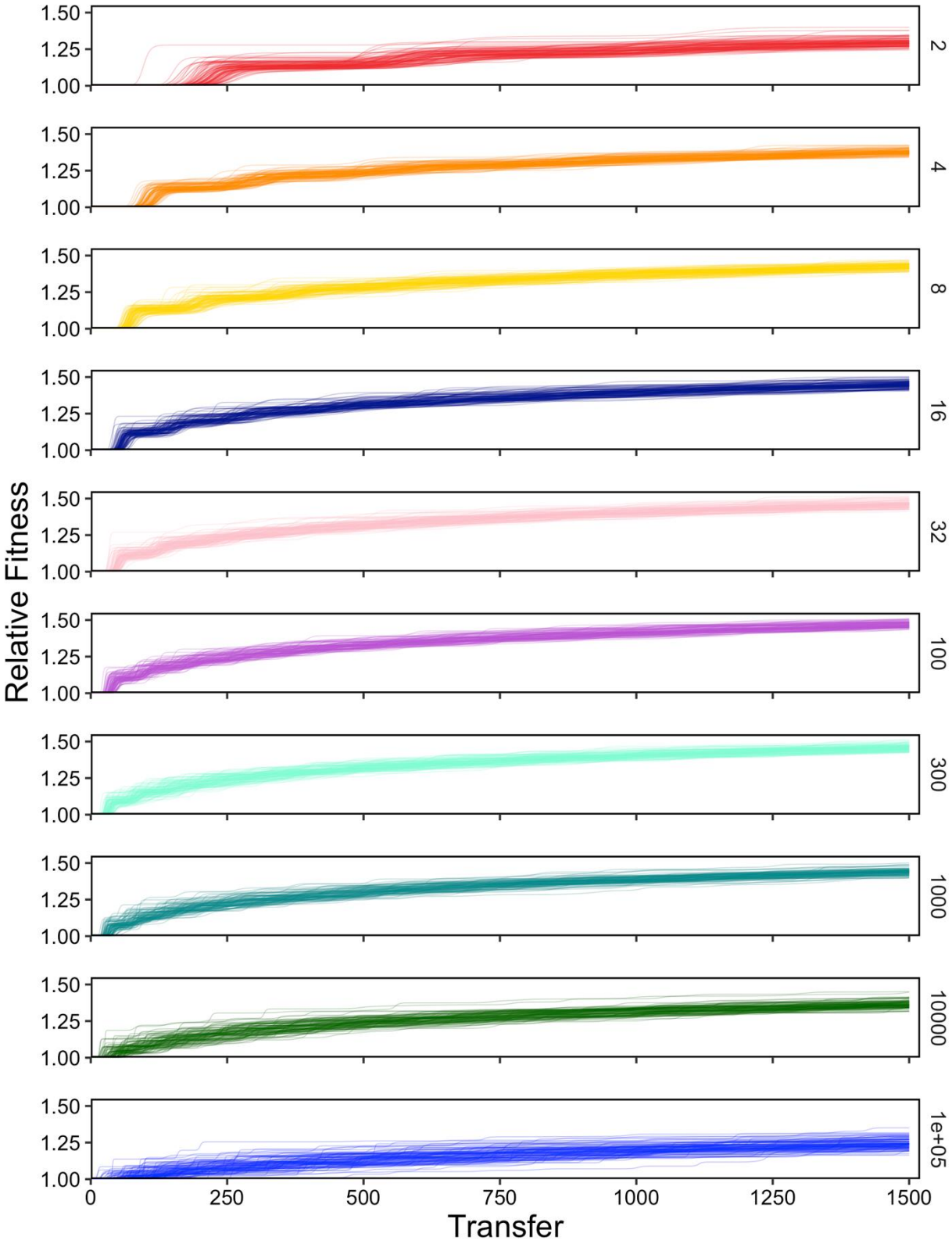

Fig. S4. Simulated relative-fitness trajectories for 100 populations evolving with various dilution factors. Trajectories for the grand means are shown in Fig. 7.

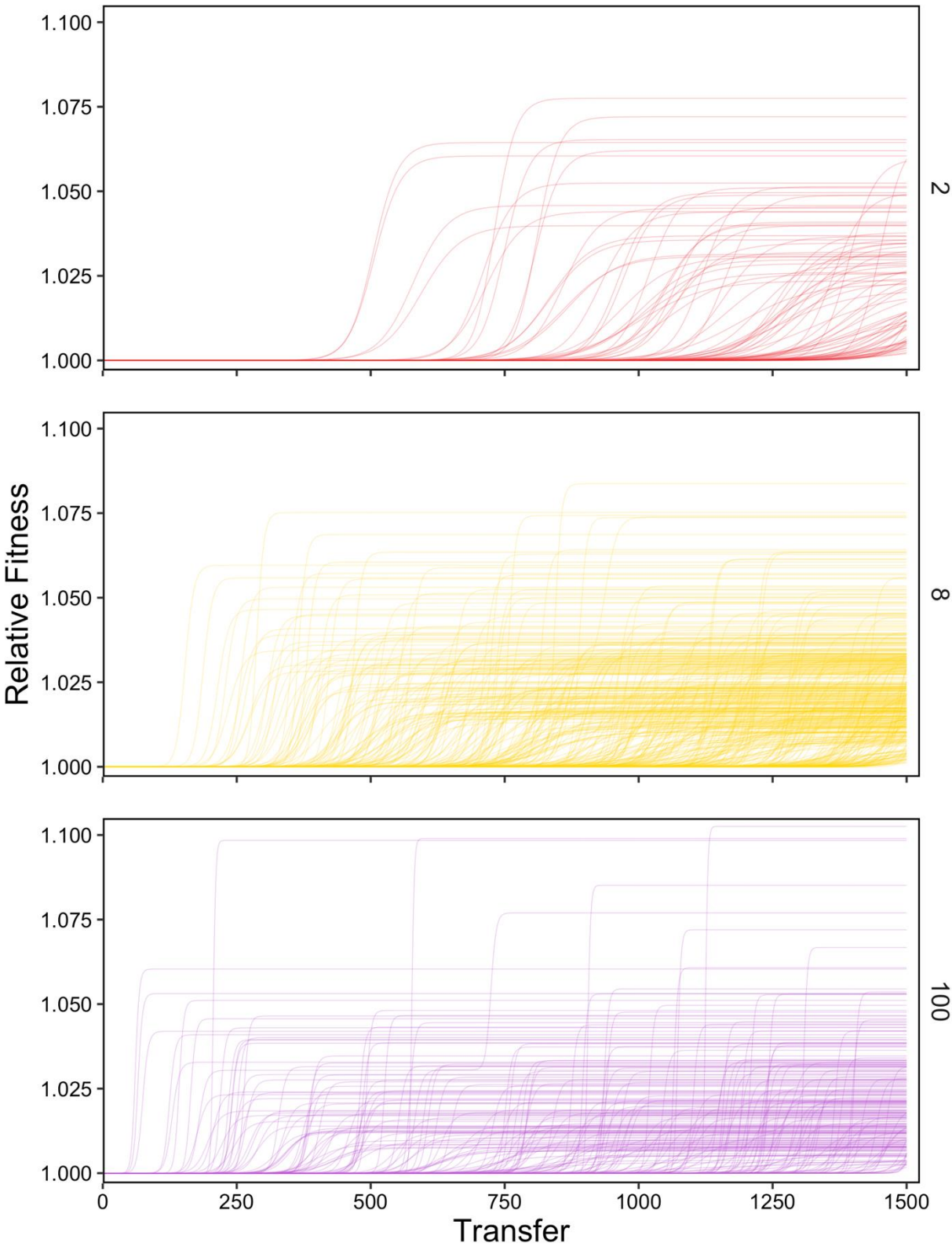

Fig. S5. Simulated relative-fitness trajectories for 10,000 populations evolving under a mutation-limited regime with three dilution factors. Note the steeper trajectories leading to similar fitness gains at the higher dilutions. Trajectories for the grand means are shown in Fig. 8.

Table S1. Relative fitness of clones used to found aberrant populations in the marker-divergence experiments.

Clone pair	Mean fitness	Mean ln fitness	df	t_s	p
–3 vs +3	0.983	–0.017	21	–4.066	0.0006
–5 vs +5	1.041	0.040	21	13.961	<0.0001

We competed each member of a founding clone pair against the reciprocally marked ancestor, and the competition assays were paired. We calculated the relative fitness of a founding pair as the ratio of each clone's fitness relative to the ancestor. We replicated the paired competitions 22 times for each clone pair. We ran two-tailed paired *t*-tests on the ln-transformed fitnesses. Each comparison is highly significant and in the direction consistent with the initial divergence in the marker ratios (Fig. 2).

Table S2. Comparison of times to divergence between the four dilution treatments in the marker-divergence experiments.

Treatment comparison	*p*
2-fold vs 8-fold	0.0079
2-fold vs 100-fold	0.0050
2-fold vs 1000-fold	0.0050
8-fold vs 100-fold	0.0122
8-fold vs 1000-fold	0.0051
100-fold vs 1000-fold	0.0146

We performed two-tailed Wilcoxon's signed-ranks tests to compare the times to divergence (*TD*s) under the four dilution treatments. As explained in the text, two aberrant trajectories were excluded in each treatment; these tests are based on the remaining 10 trajectories in each treatment. All of the comparisons are significant even after a table-wide sequential Bonferroni correction ($p < 0.05$).

Table S3. ANOVA of fluctutations in marker ratios prior to the onset of divergence associated with selective sweeps.

Source	SS	df	MS	F_s	p
Treatment	0.1278	3	0.0426	1.9677	0.1191
Error	5.9744	276	0.0216		
Total	6.1022	279			

We calculated the absolute value of the $\log_2$-transformed change in the ratio of the two marked strains for the first 7 consecutive sample pairs (3-day intervals through day 21) for 10 populations in the 4 dilution treatments (excluding the two aberrant populations in each treatment). By day 24, some populations exhibited systematic divergence in marker ratios caused by selective sweeps. The grand mean and standard deviation of these 280 early fluctuations were 0.1986 and 0.1479, respectively. The ANOVA shows no significant effect of the dilution treatment on the magnitude of these early fluctuations.

Table S4. Comparison of fitness measured in "Home" and "Away" environments of bacteria that evolved for 150 transfers under the four dilution treatments.

Treatment	Mean ln fitness Home	Mean ln fitness Away	df	t_s	p
2-fold	0.2124	0.0537	11	7.5832	<0.0001
8-fold	0.1334	0.0910	11	4.2304	0.0007
100-fold	0.1199	0.1392	11	–2.6305	0.0234
1000-fold	0.1065	0.1355	11	–3.7277	0.9983

We isolated clones at the end of the 150-transfer experiment from all of the populations in the four dilution treatments. Each evolved clone competed against the reciprocally marked ancestral strain under both the same dilution regime in which it evolved (Home) and the common 100-fold dilution regime (Away). We ran paired *t*-tests to compare the mean ln-transformed fitness values in the two environments. The tests were one-tailed in all cases except the 100-fold dilution regime, given the expectation that fitness would be higher at Home than Away; the environments are identical for the 100-fold regime, and so that test was two-tailed. Note that the reported *p*-value is high for the 1000-fold regime because the difference was opposite to that expectation.

Table S5. Comparison of final fitness of bacteria that evolved for 150 transfers under the 8-, 100-, and 1000-fold dilution treatments.

Treatment comparison	df	t_s	p
8-fold vs 100-fold	11	–4.4639	0.0010
8-fold vs 1000-fold	11	–2.2941	0.0425
100-fold vs 1000-fold	11	0.2500	0.8072

We competed the evolved clones against the reciprocally marked ancestors in the common environment (100-fold dilution), with 5-fold replication, and we calculated the mean ln-transformed fitness value for each population. We ran two-tailed paired *t*-tests to compare the treatments shown.

Table S6. Comparison of fitness changes between transfers 90 and 150 in bacteria that evolved under the 8-, 100-, and 1000-fold dilution treatments.

Treatment comparison	*p*
8-fold vs 100-fold	0.3013
8-fold vs 1000-fold	0.3394
100-fold vs 1000-fold	1

We performed two-tailed Wilcoxon's signed-ranks tests to compare the change in mean ln-transformed fitness values from 90 to 150 transfers in the treatments shown.

Table S7. Comparisons of experimental and simulated times to divergence.

Regime (*D*)	Mean Experimental *TD*	Mean Simulated *TD*	*p*
2	85.2	150.0	0.0001
8	68.4	86.7	0.0445
100	42.3	42.9	0.9696
1000	30.6	32.1	0.7269

For these comparisons, we trimmed the simulated data to match the experimental data. Thus, we used only 10 randomly chosen replicates of the simulated populations and the data from every third transfer in these calculations. For the 2-fold dilution regime, one experimental replicate had not diverged by day 150, and its time to divergence (*TD*) was recorded as 150. In the simulated dataset, none of the 10 replicates had diverged by day 150 (in fact, only 2 of the 100 replicates diverged before day 150), and so for consistency we also used day 150 for them. We compared the experimental and simulated populations using two-tailed Mann-Whitney tests. They differed significantly only for the 2-fold dilution regime after a table-wide sequential Bonferroni correction.

Table S8. Change in mean fitness in simulated populations between transfers 90 and 150 under three dilution regimes.

Regime (*D*)	Mean change	St. dev.	*p*
8	0.0208	0.0265	
			<0.0001
100	0.0572	0.0237	
			<0.0001
1000	0.0476	0.0261	

We simulated 100 replicate populations for each dilution regime. We compared each treatment with the adjacent treatments (above and below) using a two-tailed Mann-Whitney test. The difference between the 8- and 1000-fold dilution regimes was also highly significant ($p < 0.0001$).

Table S9. Mean fitness in simulated populations after 1500 transfers under ten dilution regimes.

Regime (*D*)	Mean fitness	St. dev.	*p*
2	1.2981	0.0278	
			<0.0001
4	1.3780	0.0179	
			<0.0001
8	1.4252	0.0181	
			<0.0001
16	1.4491	0.0215	
			0.0016
32	1.4600	0.0215	
			0.0013
100	1.4689	0.0175	
			<0.0001
300	1.4578	0.0192	
			<0.0001
1000	1.4390	0.0200	
			<0.0001
10^4	1.3655	0.0253	
			<0.0001
10^5	1.2435	0.0342	

We simulated 100 replicate populations for each dilution regime. We compared each treatment with the adjacent treatments (above and below) using a two-tailed Mann-Whitney test. All tests were significant ($p < 0.05$) after a table-wide sequential Bonferroni correction.

Table S10. Mean time to divergence in simulated populations under ten dilution regimes.

Regime (*D*)	Mean *TD*	St. dev.	*p*
2	236.65	61.02	
			<0.0001
4	135.01	55.66	
			<0.0001
8	81.78	29.17	
			<0.0001
16	64.09	20.52	
			<0.0001
32	53.22	15.15	
			<0.0001
100	43.98	14.67	
			<0.0001
300	36.11	9.98	
			0.6571
1000	35.75	10.67	
			0.0024
10^4	40.68	13.31	
			<0.0001
10^5	76.25	44.60	

We simulated 100 replicate populations for each dilution regime. We compared each treatment with the adjacent treatments (above and below) using a two-tailed Mann-Whitney test. All tests were significant ($p < 0.05$) after a table-wide sequential Bonferroni correction except for one (D = 300 versus D =1000).

Table S11. Change in mean fitness between transfers 1000 and 1500 in simulated populations under ten dilution regimes.

Regime (*D*)	Mean fitness	St. dev.	*p*
2	0.0511	0.0191	
			0.1743
4	0.0489	0.0157	
			0.0806
8	0.0520	0.0148	
			0.8834
16	0.0520	0.0120	
			0.9338
32	0.0527	0.0132	
			0.6583
100	0.0529	0.0113	
			0.2621
300	0.0514	0.0106	
			0.7582
1000	0.0521	0.0131	
			0.1494
10^4	0.0492	0.0166	
			0.0169
10^5	0.0433	0.0231	

We simulated 100 replicate populations for each dilution regime. We compared each treatment with the adjacent treatments (above and below) using a two-tailed Mann-Whitney test. None of the comparisons were significant after a table-wide sequential Bonferroni correction.

Table S12. Number of populations with surviving beneficial mutations and grand mean fitness after 1500 transfers in 10,000 simulated populations evolving with a low rate of beneficial mutations.

Regime (*D*)	Runs with surviving beneficial mutations	Mean fitness	*p*
2	91	1.000255	
			<0.0001
4	346	1.000956	
			0.0942
8	440	1.001097	
			0.5669
16	459	1.001049	
			0.0010
32	353	1.000800	
			<0.0001
100	240	1.000542	
			<0.0001
300	97	1.000214	
			0.0886
1000	64	1.000154	
			<0.0001
10^4	8	1.000018	
			0.0079
10^5	0	1.000000	

We simulated 10,000 replicate populations for each dilution regime. We scored populations as having a surviving beneficial mutation if the ancestral genotype's final frequency was <10%. We compared the mean fitness of each treatment with the adjacent treatments (above and below) using a two-tailed Welch's *t*-test. The comparisons between consecutive regimes were significant ($p < 0.05$) after a table-wide sequential Bonferroni correction except for the three *p* values shown in italics. Overall, mean fitness was highest in the 8-fold dilution regime, followed closely by the 16- and 4-fold regimes, and it declined in a consistent manner at both lower and higher dilution factors. Thus, comparisons of the mean fitness values for the $D = 8$ and $D = 2$ regimes, and for the $D = 8$ and $D = 32$ regimes, were highly significant ($p < 0.0001$ and $p = 0.0001$, respectively).

Table S13. List of bacterial strains used in this study.

Strain	Treatment	Replicate	Transfer	Ara marker*
REL 606	ancestor			–
REL 607	ancestor			+
MI 762	2	1	90	–
MI 693	2	1	150	–
MI 761	8	1	90	–
MI 692	8	1	150	–
MI 759	100	1	90	–
MI 739	100	1	150	–
MI 758	1000	1	90	+
MI 689	1000	1	150	+
MI 766	2	2	90	+
MI 697	2	2	150	+
MI 765	8	2	90	–
MI 696	8	2	150	–
MI 764	100	2	90	+
MI 695	100	2	150	+
MI 763	1000	2	90	+
MI 694	1000	2	150	+
MI 770	2	3	90	+
MI 701	2	3	150	+
MI 769	8	3	90	+
MI 700	8	3	150	+
MI 768	100	3	90	–
MI 699	100	3	150	–
MI 767	1000	3	90	–
MI 698	1000	3	150	–
MI 3	all**	3	0	–
MI 15	all**	3	0	+
MI 775	2	4	90	+
MI 705	2	4	150	+
MI 774	8	4	90	+
MI 704	8	4	150	+
MI 773	100	4	90	–
MI 703	100	4	150	–
MI 771	1000	4	90	+
MI 702	1000	4	150	+
MI 779	2	5	90	–
MI 709	2	5	150	–
MI 778	8	5	90	–
MI 708	8	5	150	–
MI 777	100	5	90	–
MI 707	100	5	150	–

MI 776	1000	5	90	–
MI 706	1000	5	150	–
MI 5	all**	5	0	–
MI 17	all**	5	0	+
MI 784	2	6	90	+
MI 713	2	6	150	+
MI 783	8	6	90	–
MI 712	8	6	150	–
MI 781	100	6	90	+
MI 711	100	6	150	+
MI 780	1000	6	90	–
MI 710	1000	6	150	–
MI 788	2	7	90	+
MI 752	2	7	150	+
MI 787	8	7	90	+
MI 716	8	7	150	+
MI 786	100	7	90	+
MI 715	100	7	150	+
MI 785	1000	7	90	+
MI 714	1000	7	150	+
MI 792	2	8	90	+
MI 721	2	8	150	+
MI 791	8	8	90	–
MI 720	8	8	150	–
MI 790	100	8	90	–
MI 719	100	8	150	–
MI 789	1000	8	90	+
MI 718	1000	8	150	+
MI 796	2	9	90	–
MI 725	2	9	150	–
MI 795	8	9	90	–
MI 724	8	9	150	–
MI 794	100	9	90	+
MI 723	100	9	150	+
MI 793	1000	9	90	–
MI 722	1000	9	150	–
MI 800	2	10	90	–
MI 729	2	10	150	–
MI 799	8	10	90	+
MI 728	8	10	150	+
MI 798	100	10	90	–
MI 727	100	10	150	–
MI 797	1000	10	90	–
MI 726	1000	10	150	–
MI 804	2	11	90	–

MI 733	2	11	150	–
MI 803	8	11	90	–
MI 732	8	11	150	–
MI 802	100	11	90	–
MI 731	100	11	150	–
MI 801	1000	11	90	–
MI 730	1000	11	150	–
MI 809	2	12	90	+
MI 737	2	12	150	+
MI 808	8	12	90	+
MI 736	8	12	150	+
MI 807	100	12	90	+
MI 735	100	12	150	+
MI 810	1000	12	90	+
MI 754	1000	12	150	+

* All Ara^{-} and Ara+ strains derive from *E. coli* REL606 and REL607, respectively.

** Founding clones for populations that showed aberrant trajectories (Fig. 2) and unequal initial fitness values (Table S1).

SI References

1. R. E. Lenski, M. Travisano, Dynamics of adaptation and diversification: a 10,000-generation experiment with bacterial populations. *Proc. Natl. Acad. Sci. U.S.A.* **91**, 6808–6814 (1994).
2. P. J. Gerrish, R. E. Lenski, The fate of competing beneficial mutations in an asexual population. *Genetica* **102**, 127–144 (1998).
3. L. M. Wahl, P. J. Gerrish, I. Saika-Voivod, Evaluating the impact of population bottlenecks in experimental evolution. *Genetics* **162**, 961–971 (2002).
4. C. D. Kemp, A. W. Kemp, Poisson random variate generation. *J. Roy. Stat. Soc. C* **40**, 143–158 (1991).
5. M. J. Wiser, N. Ribeck, R. E. Lenski, Long-term dynamics of adaptation in asexual populations. *Science* **342**, 1364–1367 (2013).